Fall 2015

Formation and evolution of Spinel in aluminum killed calcium treated linepipe steels

Obinna Adaba

Department:

FORMATION AND EVOLUTION OF SPINEL IN ALUMINUM KILLED CALCIUM TREATED LINEPIPE STEELS

by

OBINNA M. ADABA

A THESIS

Presented to Graduate Faculty of the

MISSOURI UNIVERSITY OF SCIENCE AND TECHNOLOGY

In Partial Fulfillment of the Requirements for the Degree

MASTER OF SCIENCE IN METALLURGICAL ENGINEERING

2015

Approved by

Ronald J. O'Malley, Advisor
Von L. Richards
Simon N. Lekakh

PUBLICATION THESIS OPTION

This dissertation consists of two manuscripts prepared for conference proceedings. Pages 20-34 have been presented at the 9th international clean steel conference. The manuscript on pages 35-51 is intended for presentation at the AISTech 2016 conference.

ABSTRACT

Magnesium aluminate (Spinel) inclusions have been observed to cause hook crack in line pipe steels. These inclusions are typically formed during liquid steel processing at the ladle metallurgy furnace (LMF) and subsequently modified by calcium to form less harmful liquid inclusions. Unfortunately, spinel inclusions are still sometimes observed in samples taken from the tundish and coil after calcium treatment.

The formation and evolution of spinel inclusions during liquid steel processing at two industrial mini mills was investigated by analysis of lollipop samples taken at different stages of the steelmaking process. The effect of reoxidation on the formation of spinels after calcium treatment was also investigated by thermodynamic calculations and laboratory experiments.

The results showed that spinel inclusions are first formed in liquid steel after desulfurization and by the reaction between dissolved aluminum in liquid steel and MgO in the ladle slag. These inclusions were modified by calcium to both liquid and solid calcium aluminates. Also observed after calcium treatment, was the formation of MgO rich and CaS inclusions. During liquid steel transfer to the tundish, evidence of reoxidation and ability of CaS to act as a source of calcium to modify inclusions formed during reoxidation was observed. Analysis of the results from the laboratory experiment showed that with sufficient magnesium in steel (about 4ppm) spinel inclusions can be formed during liquid steel reoxidation. The results also showed that spinel inclusions observed after reoxidation of calcium treated steel are larger in size than those observed prior to calcium treatment. The modification of spinels by calcium and reformation after liquid steel reoxidation was verified by thermodynamic calculations.

ACKNOWLEDGEMENTS

I wish to extend my profound appreciation to the following individuals for their guidance and technical support during the course of attaining my Master's degree here at Missouri University of Science and Technology.

I am immensely grateful and thankful to my advisors Dr. Ronald J. O'Malley, Dr. Von L. Richards, and Dr. Simon N. Lekakh for the technical and moral support given to me during the course of carrying out this work and for making me a better individual.

I am grateful to the Peaslee Steel Manufacturing Research Center (PSMRC), and participating member companies for providing the resources to enable me carry out this work.

I wish to thank all the graduate and undergraduate students who assisted me during the course of this work.

My sincere gratitude also goes to the Late Dr. Kent Peaslee for his support and guidance. You will always be remembered.

Finally, I thank my parents and siblings for their guidance and support throughout this work and my entire life.

TABLE OF CONTENT

Page

LIST OF ILLUSTRATIONS

LIST OF TABLES

SECTION
1. INTRODUCTION

1.1. OVERVIEW

Oil country tubular goods (OCTG) or line pipe steels are used in the oil and gas industry to extract and transport natural gas. These steels are aluminum killed and calcium treated. Table 1.1 shows the typical composition for the steel grade examined in this study. During welding at the pipe manufacturing location, hook cracks have been observed to form and often lead to pipe rejection. Hook cracks are fractures that take the form of a hook or "J" shape and are typically observed in the vicinity of a weld line [7] (fig 1.1).

OCTGs are manufactured from steel coils produced by the continuous casting and hot rolling steelmaking process. These coils are shipped from the steelmaking facility to the pipe manufacturing location where they are uncoiled, slit and welded by electric resistance welding (ERW) to produce the pipes [10]. Microscopic investigation of a pipe sample that contained hook cracks, revealed the presence of spinel inclusions as the cause of the cracks (fig 1.2). These inclusions are stable at steelmaking temperatures (Mpt.2135˚C) and are produced during liquid steel processing. They have an irregular shape and when present in the product, their surface acts as a preferential site for crack nucleation and propagation.

The goal of this research was to investigate the formation and evolution of spinel inclusions during liquid steel processing of line pipe steels. Specific attention was given to the time of formation of spinels and the source of magnesium in the liquid steel. The ability of calcium to modify these inclusions, and the effect of liquid steel reoxidation on the formation of spinels were also investigated. Samples for inclusions analysis were taken from industrial mini mills and laboratory experiments also conducted to verify developed thermodynamic models.

Table 1.1: Steel Composition for Line pipe Steels

Element	C	Al	Si	Mn	S	Ca
Amount,wt.%	0.2	0.04	0.2	1	0.003	0.002

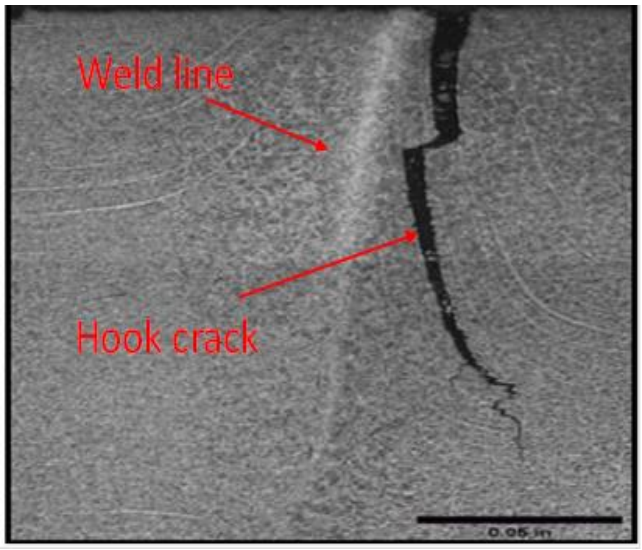

Figure1.1: Hook Crack in an OCTG. Crack observed adjacent to the weld line and formed during the welding process [7].

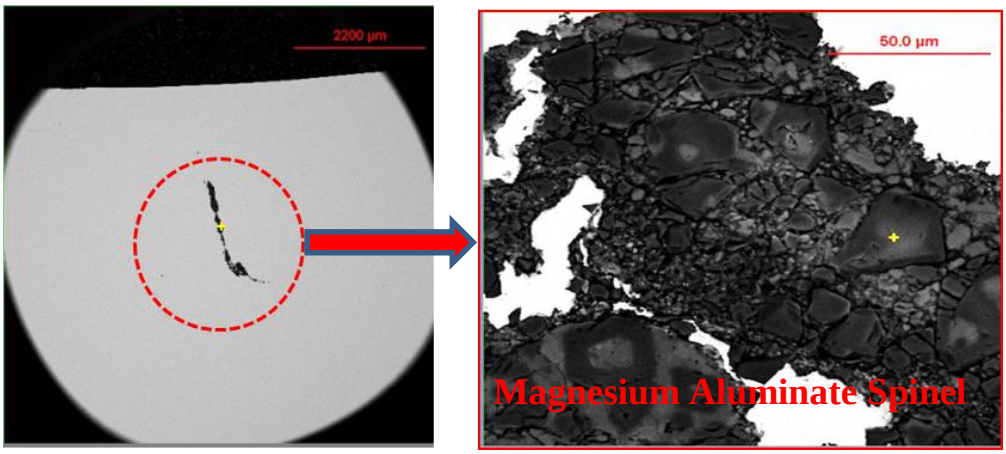

Figure 1.2: Spinel inclusions observed in linepipe sample containing hook crack.

1.2. STEELMAKING AND LINE PIPE PRODUCTION

Steel products are produced via two main routes namely basic oxygen furnace (BOF) and electric arc furnace (EAF) route. The main difference between these steel making methods is in the type of raw materials used and the method of heating. In BOF, about 70% of the raw material is liquid iron produced in a blast furnace where decarburization is performed by blowing oxygen into the melt. In the EAF route, the raw materials are predominantly scrap metal and both electrical energy and oxygen injection is used in melting the scrap materials. Both processes can further be divided into 3 stages; primary steelmaking, secondary steelmaking, and continuous casting.

Primary steelmaking is the first stage of the steelmaking process where essential raw materials are added into a furnace and the steel brought to the desired temperature for further processing. At this stage, Carbon and other impurities such as phosphorus and manganese are removed from the melt via gaseous and oxide products produced from their reaction with oxygen. Eqns. 1 to 6 represent some of the possible reactions occurring at this stage of steelmaking. At the end of primary steelmaking, the oxygen content in the steel is around 400-1000 parts per million (ppm). With this amount of oxygen, continuous casting of quality steel is almost impossible as the low oxygen solubility in solid steel (about 4ppm) causes CO formation during cooling and solidification which ultimately produces blow holes in the final structure.

$$[C]+\frac{1}{2}O_{(g)} = CO \quad (1)$$

$$[C]+ O_{2(g)} = CO_{2(g),} \quad (2)$$

$$[Si] + 2[O] = (SiO_2) \quad (3)$$

$$2[P] + 5[O] = (P_2O_5) \quad (4)$$

$$[Mn] + [O] = (MnO) \quad (5)$$

$$[Fe] + [O] = (FeO) \quad (6)$$

Liquid steel deoxidation is achieved at the secondary or ladle metallurgy furnace (LMF). At this stage, the steel from the EAF/BOF is tapped into a ladle and deoxidizers added into the melt. Basic slags are also used in ensuring a reducing environment in the melt. It is important that the transfer of primary steelmaking furnace slags during tapping be minimized as this can create oxidizing conditions leading to poor alloy recoveries and phosphorus reversion. The LMF is also employed to perform liquid steel desulfurization, alloying, temperature and steel bath homogenization, and non-metallic inclusion control. At the end of the process, the liquid steel is transferred through protective refractory shrouds to a tundish and finally to the mold for continuous casting.

Continuous casting is the final stage in liquid steel processing where the liquid steel cools and solidifies in a mold. At this stage, the liquid steel from the LMF is transferred to a tundish which acts as a reservoir of molten metal for the mold. Continuous casting is a method where the liquid steel is cast into a billet, bloom or slab for further processing [24] and this method provides several advantages over ingot casting

which include, reduced time and cost for steel production, and improved yield and quality. Initial solidification of the liquid steel starts in the mold and continues on through a series of vertical and horizontal rolls that support and shape the metal to the desired form for further processing and handling.

For line pipe steels, the slabs that exit the caster are further reheated, rolled, and coiled for transportation to the pipe manufacturing station. At the pipe manufacturing station, the metal is uncoiled, slit, roll formed and welded by ERW to produce the pipes. Figure 1.3 is a schematic of the pipe manufacturing process for line pipe steels. It is during the process of welding where there is combined action of mechanical deformation and heating, that hook cracks are formed [10]. Although these cracks have been related to manganese sulfide inclusions in the past [12], spinel inclusions have recently been observed after microscopic investigation of samples containing the cracks.

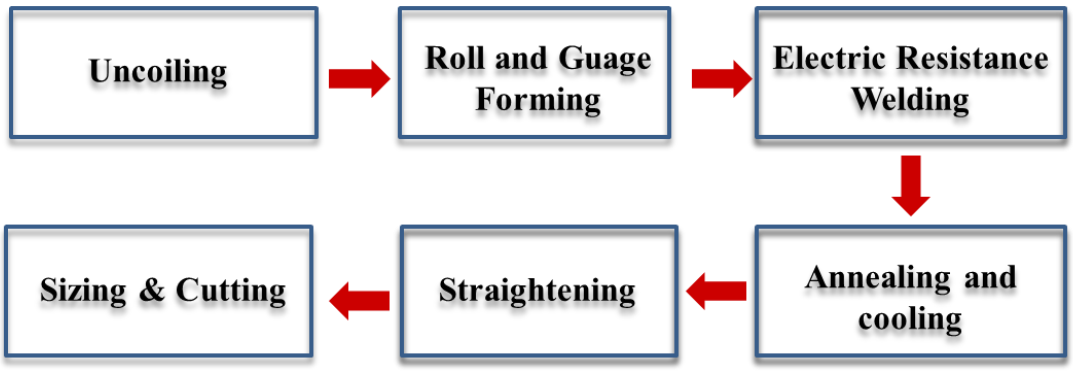

Figure 1.3: Stages during the pipe manufacturing of line pipes.

1.3. NON-METALLIC INCLUSIONS AND SPINEL

Non-metallic inclusions are microscopic inorganic compounds dispersed in liquid steel during processing and are also found in steel products. They affect the stability of the casting process by clogging submerged entry nozzles (SEN) and also the quality of the steel product; they have been known to affect properties such as the mechanical strength, toughness, corrosion and surface quality of the product [21,22].

Important inclusion characteristics are their size, composition, amount, and distribution [21]. Large inclusions should always be avoided as they promote crack formation. Table 1.2 shows the critical size of inclusions for different steel grades. Oxide

inclusions such as alumina promote clogging of SENs. and affect the mechanical strength of the product while manganese sulfide inclusions (MnS) cause hot tearing [12]. The toughness of metals has also been observed to be affected by the amount and distribution of inclusions and increases with increasing distance between inclusions.

While for the most part non-metallic inclusions are harmful to the steelmaking process and quality of the product, they are also beneficial in certain applications when their characteristics are controlled. In resulfurized steel grades, the presence of MnS and complex calcium alumina silicates has been observed to improve machinability [22]. The term "oxide metallurgy" has been used to describe the ability of discrete oxide inclusions to improve mechanical strength through promoting grain refinement [21].

Table 1.2: Critical inclusion size for different steel products [18]

Steel Product	**Maximum inclusion size (μm)**
Automotive and deep drawing sheet	100
Drawn and Ironed cans	20
Line pipe	100
Bearings	15
Tire cord	10
Heavy plate steel	13
Wire	20

1.3.1. Types of Inclusions. Nonmetallic inclusions in steel can be composed of oxides, sulfides, carbides, nitrides [22] and or composed of entrained exogenous materials. They can be simple oxides such as the alumina and silica or they can also be complex in nature; consisting of more than one compound and or multiple phases. The type of inclusion found in the steel depends on the steel grade. In aluminum killed steels, alumina inclusions are produced while complex manganese silicates are found in steels deoxidized using manganese and silicon. Figure 1.4 shows different types of inclusions observed in steel.

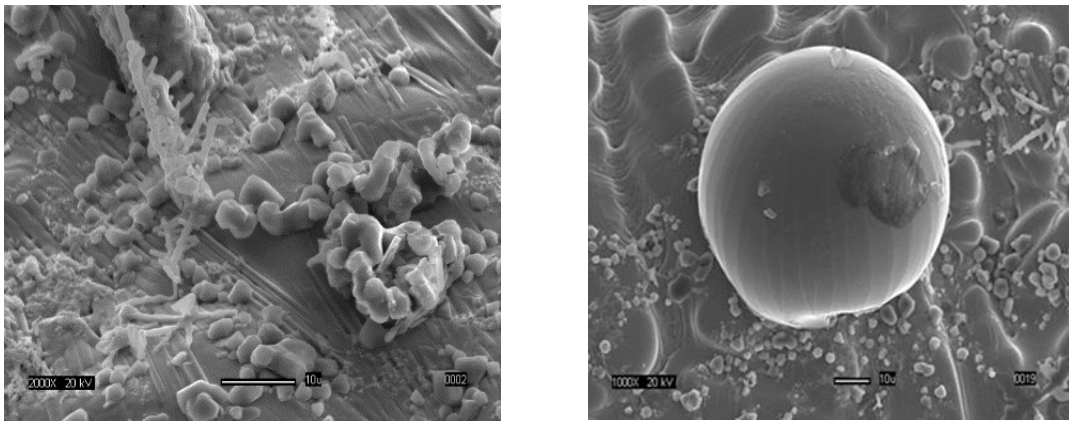

(a) (b)

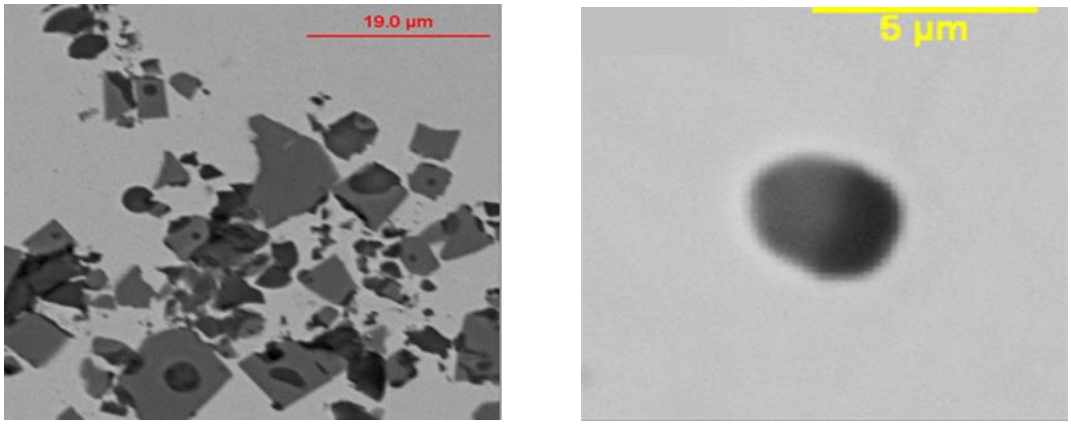

(c) (d)

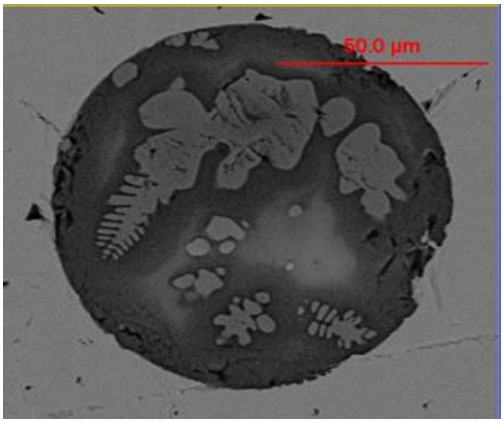

(e)

Figure 1.4: Different types of inclusions observed in steel. (a) Alumina cluster, (b) calcium aluminate, (c) Titanium nitride, (d) Complex calcium sulfide-calcium aluminate, (e) Manganese silicate complex inclusion [PSMRC and ArcelorMittal Global R&D]

1.3.2. Classification of Inclusions. Non-metallic inclusions can be classified according to their mode of formation, size, and or inclusion composition. Endogenous inclusions are compounds formed by reactions occurring within the liquid steel. This type of inclusions include deoxidation products and are formed as a consequence of current steelmaking practice and hence, unavoidable. Endogenous inclusions can further be divided into primary and secondary endogenous inclusions. Primary endogenous inclusions are formed at liquid steelmaking temperatures while secondary endogenous inclusions on the other hand are formed during cooling and solidification of the liquid steel. These inclusions include carbides and nitrides formed from precipitation.

Exogenous inclusions are foreign materials that become entrained in the liquid steel during processing. They are present due to mechanical and or chemical interactions between the steel and surrounding material. These inclusions are mainly refractory or slag materials used to contain the liquid steel and provide protection from the surrounding environment. They are typically larger than endogenous inclusions (greater than 100μm) and are also known as macro inclusions.

1.3.3. Formation and Growth of Inclusions. Liquid steel deoxidation is typically carried out at the early stages of LMF using a metal having stronger affinity for oxygen than iron. Aluminum represents the most commonly used deoxidizer because of its ability to produce steel having very low oxygen potential. Figure 1.5 is the deoxidation equilibria for aluminum in liquid steel at 1600 ˚C. At 0.05 wt.% aluminum, the soluble oxygen content is about 4ppm. When aluminum is added into liquid steel, it reacts with the dissolved oxygen to produce alumina inclusions (eq.7).

$$2[Al] + 3[O] = (Al_2O_3), \quad (7)$$

$$\Delta G^o\,(J/mol) = -RT \ln K == 403163\text{-}130.5T \text{ [29]} \quad (8)$$

$$\ln(K) = \frac{a^{Al_2O_3}}{h_{Al}^2 \cdot h_O^3} \quad (9)$$

$h_{Al} = f_{Al} \cdot [Al]$ and $h_O = f_o \cdot [O]$

$2lnf_{Al} = 2e_{Al}^{Al}[Al] + 2e_{Al}^{O}[O] + 2\sum e_{Al}^{i}[O] + 2\rho_{Al}^{Al,O}$[Al][O]

$3lnf_O = 3e_O^O[O] + 3e_O^{Al}[Al] + 3\sum e_O^i[Al] + 3\rho_O^{Al,O}$[Al][O]

Where “h” is the henrian activity and “f” is the interaction coefficient. “e” and “ρ” represent the first and second order interaction coefficients respectively.

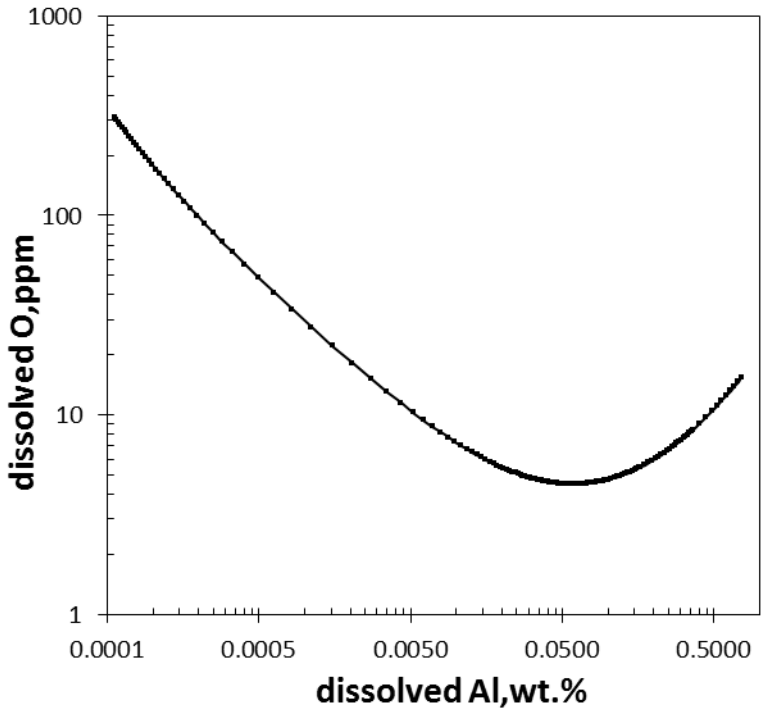

Figure 1.5: Aluminum deoxidation equilibria in liquid steel containing 0.2wt.% C. Plot calculated using Factsage 6.4 and FactPS, FTMisc, and FToxid databases.

Inclusions nucleate in liquid steel when the thermodynamic driving force (Gibbs free energy) of their formation reaction is negative. From classical thermodynamics, the free energy for the homogenous nucleation of a spherical particle is given as eq. 10. Where “ΔG_v” is the volume free energy and is related to the degree of super saturation (eq. 11). The degree of super saturation is the ratio of the concentration of reacting elements to their equilibrim concentration and must be greater than one for nucleation to occur. Also, the higher the degree of super saturation, the driving increases and more particles nucleate.

After nucleation of inclusions, growth occurs when the inclusions have reached a critical size that is given by eq.12 for a spherical partical. In liquid steel, growth of inclusions occur by ostwald ripening and collision[23].

$$\Delta G = 4/3\pi r^3 \Delta G_v + 4\pi r^2 \sigma \quad (10)$$

$$\Delta G_v = -\frac{RT}{V_m} \ln \prod \quad (11)$$

$$r_c = -2\frac{\sigma}{\Delta G_v} \quad (12)$$

where $\prod$= degree of supersaturation = $\frac{Actual\ concentration\ of\ reacting\ elements}{Equilibrium\ concentration\ of\ reacting\ elements}$

1.3.4. Inclusion Control Methods. Non-metallic inclusions are removed from the steel bath by absorption into the ladle slag [27,28]. This mechanism involves transportation to the slag interface, separation, and dissolution into the slag [27]. Floatation of inclusions to the slag by gravity is described by stokes equation (eq. 13). Where "u" is the upward velocity, Δp is the density difference between liquid steel and inclusion, "d" is the diameter of the particle, "g" is acceleration from gravity and "μ" is the viscosity of the molten steel.

$$U = \frac{gd^2\Delta p}{18\mu} \quad (13)$$

For a 100μm alumina inclusions (density = 3000Kgm^{-3} [27]), the time taken for the inclusions to float a distance of 5 meters from the slag interface is approximately 38mins. Removal of inclusions therefore from a typical 180ton steelmaking ladle requires liquid significant steel processing times. To aid in the removal of inclusions, the liquid steel is stirred with argon gas which is introduced through porous plugs at the bottom of the ladle. The inclusions get attached to the gas bubbles and are agglomerated and subsequently transported to the slag interface.

Because complete removal of all inclusions is not possible, calcium is typically added at the end of the secondary metallurgy to modify the remaining oxide inclusions [3,8,11,13]. This process is commonly used for alumina inclusions and alters the composition and shape of the inclusions; changing them from irregular solid to spherical liquid inclusions. Figure 1.6 shows the range of inclusion compositions that can be formed during calcium modification of alumina inclusions. At steel making temperatures of 1600 ˚C and at around 50 wt.% CaO, a liquid calcium aluminate inclusion is formed. This

liquid inclusion does not clog SENs and also has less detrimental effects on mechanical properties because of its spherical shape. The liquid window is the target area for calcium treatment.

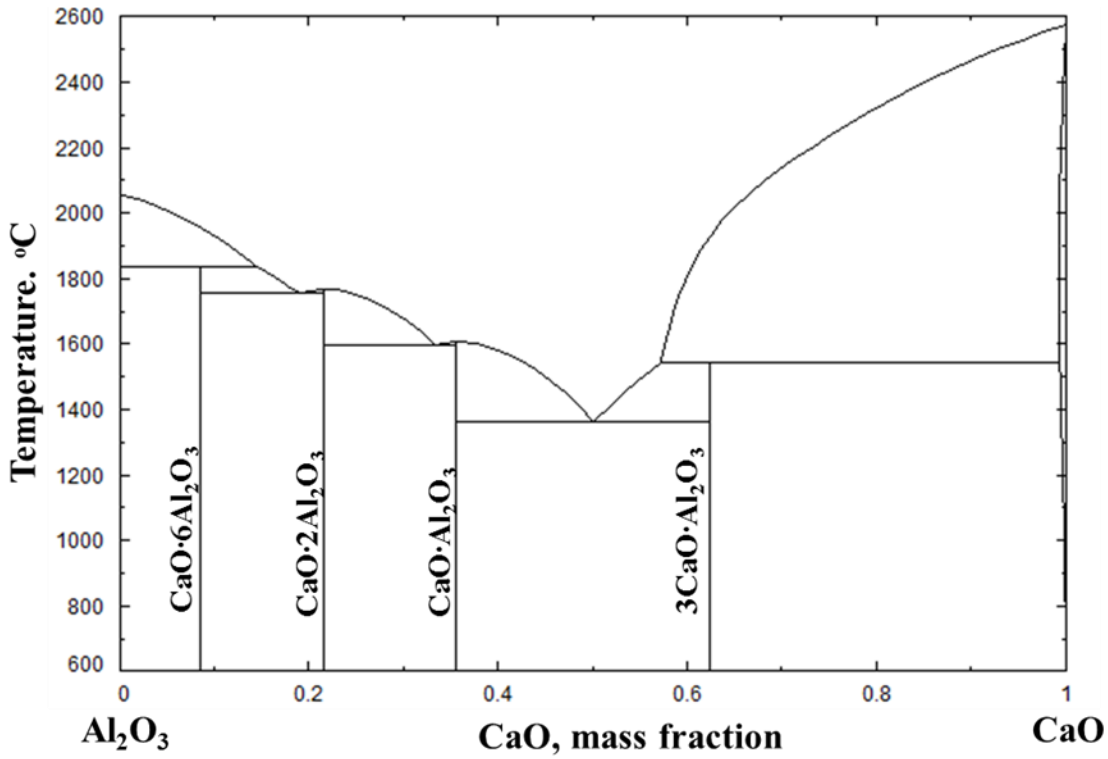

Figure 1.6: Calcium modification of alumina inclusions. At steelmaking temperatures and about 0.5 mass fraction CaO, liquid inclusions are formed. calculated using Factsage 6.4 and FactPS, FTMisc, and FToxid databases.

1.3.5. Magnesium Aluminate Inclusions (Spinel). Spinels are a family of compounds having the general formula (AB_2X_4) where 'A' and 'B' represent cations and 'X' is an anion. Examples of compounds belonging to this group include manganese aluminate, magnesium ferrite, and magnesium aluminate. Magnesium aluminate inclusions are a specific spinel compound with aluminum and magnesium as the respective cations and oxygen as the anion. They are represented by the formula ($MgO{\cdot}Al_2O_3$), have a cubic crystal structure and are solid at steelmaking temperatures. Figure 1.7 is a schematic of the crystal structure of spinel showing the respective positions of aluminum, magnesium, and oxygen ions. Al^{3+} ions are seen to occupy

octahedral sites while Mg^{2+} ions occupy the tetrahedral sites in the structure. Figure 1.8 shows the range of MgO content in alumina where single phase spinel exists and is seen to vary from 20-30% MgO at steelmaking temperatures.

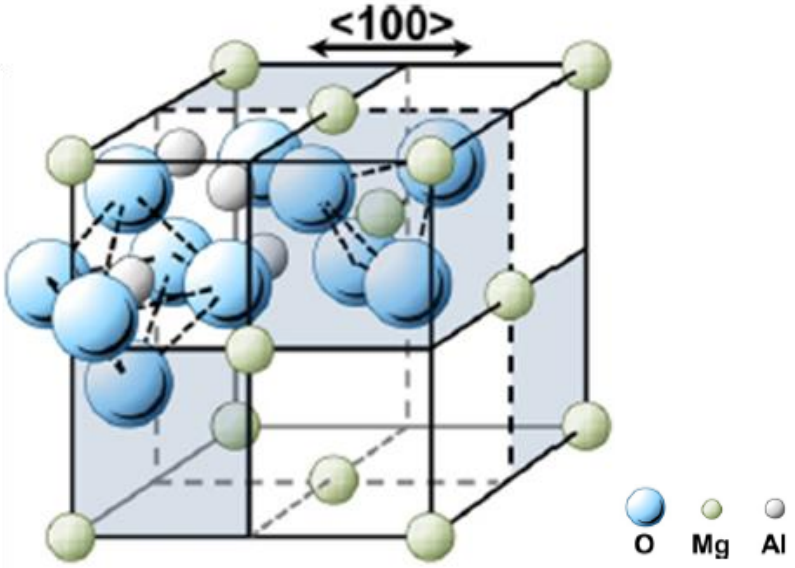

Figure 1.7: Spinel crystal structure showing the positions of the respective ions. Al^{3+} ions occupy octahedral sites while Mg^{2+} ions occupy the tetrahedral sites [26].

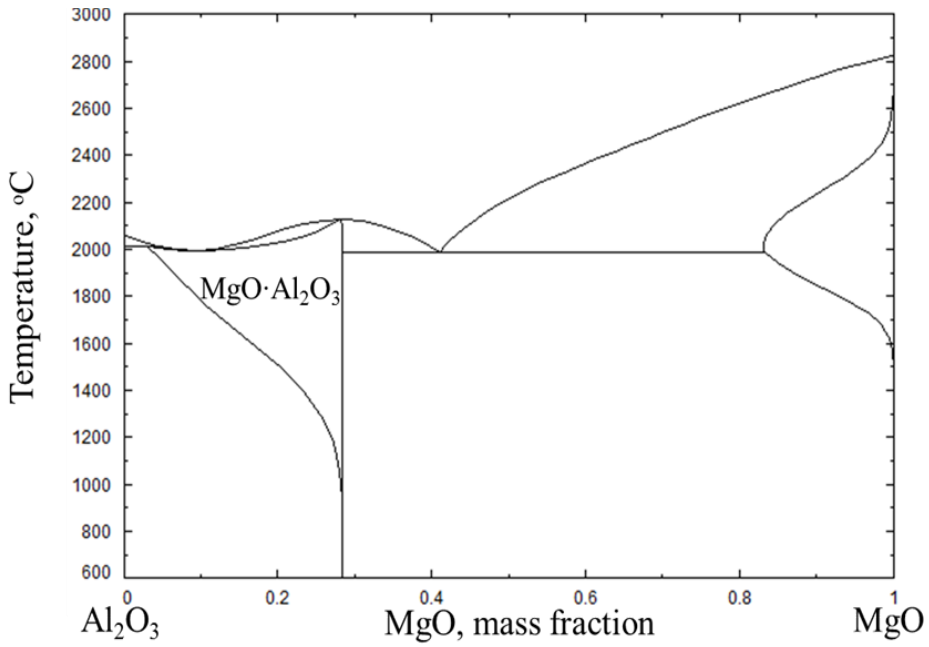

Figure 1.8: $MgO{\cdot}Al_2O_3$ phase diagram showing the compositional range of single phase spinel inclusions. calculated using Factsage 6.4 and FactPS, FTMisc, and FToxid databases

1.3.5.1. Formation of spinels. Spinel inclusions are formed by reactions between liquid steel and ladle slag or refractory, or they are formed after calcium treatment due to liquid steel reoxidation [13]. During secondary metallurgy, steel holding ladles are typically lined with magnesia carbon (MgO-C) refractories. These refractories have a high thermal conductivity and also provide high resistance to liquid steel and slag penetration [25]. To minimize dissolution of the refractory into the ladle slag, MgO saturated basic slags are typically used. Figure 1.9 shows the calculated MgO saturation for different slags using Factsage 6.4 and actual MgO content in slag from industrial mini mills. Most of the plant data is seen to be close to MgO saturation to minimize dissolution of the refractory.

In aluminum killed steel, the MgO in either the slag or refractory can be reduced by dissolved aluminum at steelmaking temperatures. Eqns. 14, shows the mechanism for this reaction. This reaction produces magnesium in solution for the formation of spinels (eqns. 15 and 16). Because magnesium is not added directly to the steel, both the slag and refractory serve as the potential sources of magnesium for spinel formation.

The exact source of the magnesium in liquid steel however, is a subject of debate [13] and some researchers proposed that spinel inclusions are formed by reactions between the dissolved aluminum and the ladle slag. This is because of the liquid to liquid kinetics being more feasible than liquid to solid reactions. However, laboratory experiments have shown that reactions between aluminum killed steel and refractories can also produce spinel inclusions in the liquid steel [15].

The aim of the first part of this research therefore focuses on the formation and evolution of spinel inclusions during secondary steelmaking and in the tundish. Comparisons are also made on the effect of different mini mill plant practices on the inclusions compositions.

$$2[Al] + 3(MgO) = (Al_2O_3) + 3[Mg] \quad (14)$$

$$[Mg] + [O] = (MgO) \quad (15)$$

$$(Al_2O_3) + (MgO) = (MgAl_2O_4) \quad (16)$$

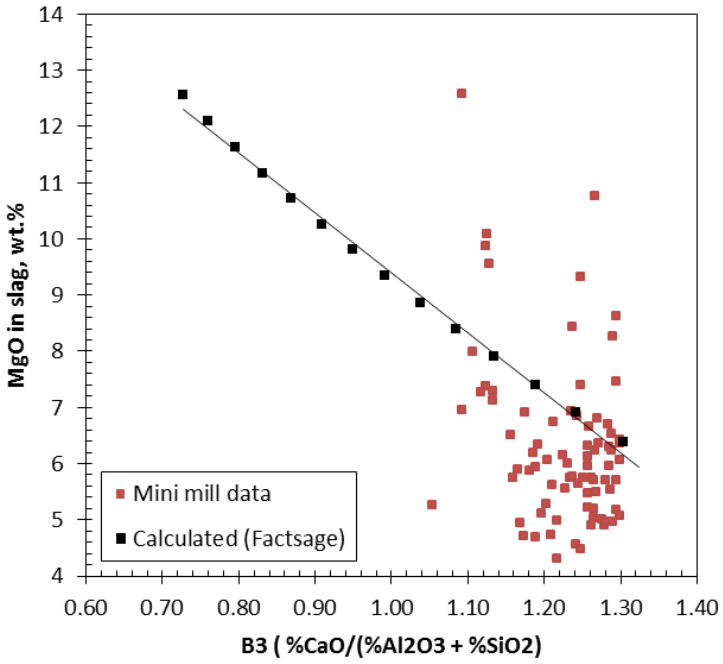

Figure 1.9: Equilibrium MgO content for different slag B3 ratios. Equilibrium line calculated using Factsage 6.4 and FactPS, FTMisc, and FToxid databases.

1.3.5.2. Formation of spinels after calcium treatment and liquid steel reoxidation. The addition of calcium has been shown to be effective in spinel modification [13]. Figure 1.10 shows the calculated Al_2O_3-MgO-CaO ternary at 1600 ˚C. At this temperature, a liquid calcium magnesium aluminate phase with MgO content up to 20% exists. Neerav Verma et al [13] studied the modification of spinels with calcium by analyzing industrial samples and also carrying out laboratory experiments. They concluded that modification of spinel by calcium was easier to achieve than modification of alumina because of the small amounts of MgO. They further proposed a mechanism where the magnesium oxide (MgO) in spinel is reduced by calcium and magnesium re-dissolves into the liquid steel (eqn. 17). Studies by Shufeng et al [20] also agreed with this proposed mechanism and in their work, they observed the formation of a calcium aluminate layer around the spinel inclusions.

Spinels have however still been observed in samples taken from the tundish and mold after calcium treatment. Neerav Verma et al proposed that these inclusions formed as a result of liquid steel reoxidation. Reoxidation of liquid steel can occur during transfer of liquid steel from the ladle to the tundish [1,13]. Based on the proposed reaction

mechanism for the calcium modification of spinel, magnesium re-dissolves into the liquid steel. After reoxidation, reformation of spinels occurs by reaction between dissolved magnesium, aluminum, and oxygen. The reaction mechanism for the reformation of spinels after liquid steel reoxidation is given by eqn. 18. Magnesium however is very volatile (Bpt. 1000˚C) and there is debate about its solubility in liquid steel [26].

The second part of this research focuses on the formation of spinel inclusions after liquid steel reoxidation. Thermodynamic models were developed and laboratory experiments performed. The method for representing the size distribution of inclusions using the population density function (PDF) is also introduced and applied to distinguish new inclusions from existing inclusion populations.

$$[Ca] + (MgAl_2O_4) = CaO{\cdot}Al_2O_3 + [Mg] \quad (17)$$

$$[Mg] + [Al] + [O] = (MgO{\cdot}Al_2O_3) \quad (18)$$

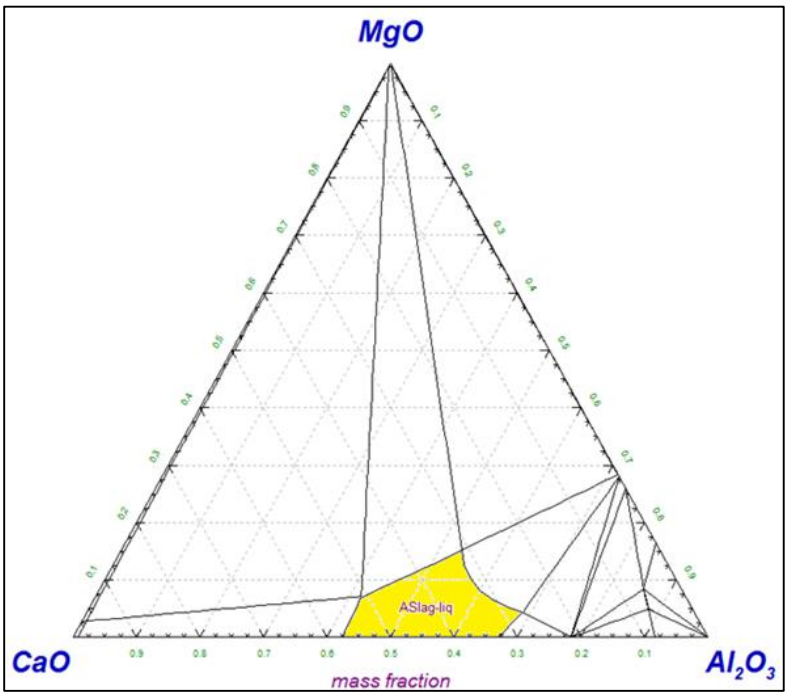

Figure 1.10: Al_2O_3-MgO-CaO ternary at 1600 ˚C. calculated using Factsage 6.4 and FactPS, FTMisc, and FToxid databases

1.4. STATEMENT OF PURPOSE

The goal of this research was to investigate the formation and evolution of spinel inclusions during liquid steel processing of line pipe steels. This research is divided into two parts. Part one deals with the formation and evolution of spinels at the LMF. Specific attention was given to the time of formation of spinels and the source of magnesium in the liquid steel. Also the ability of calcium to modify these inclusions was investigated. Part two deals with the effect of liquid steel reoxidation on the formation of spinels. Samples for inclusions analysis were taken from industry mini mills and laboratory experiments also conducted.

2. METHODOLOGY

Detailed results of the methodology used in this research can be found in the study "Improved Methodology for Automated SEM/EDS Non-Metallic Inclusion Analysis of Mini-Mill and Foundry Steels" [1].This article was published at the 2015 Association of Iron and Steel Technology (AISTech) conference proceedings. Below is a summary of the methodology.

2.1. SAMPLE PREPARATION

Lollipop samples were collected during liquid steel processing for inclusion characterization. Samples were sectioned, mounted in a resin, and ground using silicon carbide paper. Polishing was done using diamond paste to a 1μm finish. All samples were prepared in accordance with ASTM E3-11. After sample preparation, the inclusions were analyzed with automated scanning electron microscope with energy dispersive spectroscopy.

2.2. AUTOMATED FEATURE ANALYSIS (AFA)

Automated feature analysis (AFA) characterizes non-metallic inclusions based on difference in threshold values between the inclusion and the matrix. Figure 2.1 is a schematic of inclusion detection and measurement using AFA. The red areas in the figure represent an inclusion or a feature. In characterizing inclusions, an electron beam scans the sample area by moving in distances which are set by the position of the bold black dots. Once an inclusion that meets the threshold criteria is detected, it is then measured by incremental distances set by the smaller dots. The size of the inclusions is determined as the average length of eight chords measured across the inclusion. After the inclusion is measured, the average chemical composition is determined by collection of energy rays from the measured area. This technique provides the advantage of characterizing a large number of inclusions in a relatively short time and thus providing good statistical information about the inclusion population.

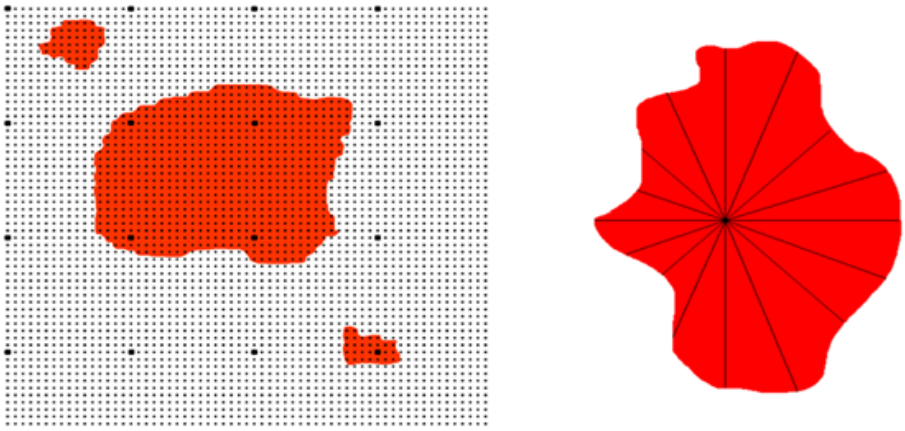

Figure 2.1**:** ASPEX detection method and area measurement method.

2.3. POST PROCESSING AND INCLUSION REPRESENTATION

AFA provides information on the inclusion size, shape, composition and amount. The data generated however, is meaningless without post processing of the data to give important information about the characteristics of the inclusion population. Methods of calculating the mass balance of elements in the inclusion and also representing the inclusion population were therefore developed and applied

2.3.1. Mass Balance Calculation. Mass balance calculations were developed to study the transfer of elemental content between the liquid steel and inclusion. Equation 11 shows the method for calculating the ppm content for each element in the inclusion.

$$M_{ppm} = \frac{\%m\, A_f\, \rho_i}{100\rho_m} \tag{11}$$

where: M_{ppm} is the mass fraction in ppm of a given element, A_f is the total inclusion area fraction, ρ_i and ρ_m are the density of the inclusion and matrix (taken to be iron) respectively, *and* $\%m$ is the areal average mass percent of a given element calculated from equation 12.

$$\%m = \frac{\sum(\%w)(A_{inclusion})}{A_{total}} \tag{12}$$

w_i is the weight percent of the given element from AFA analysis.

2.3.2. Joint Ternary. Traditional methods for representing the inclusion composition using single ternaries are subject to errors from normalization. Inclusions are typically composed of more than three elements and when represented using this form,

can lead to misinterpretation of the inclusion chemistry. Also this method provides no information on the size of the inclusions. A method was therefore developed to represent the inclusion composition and size using joint ternaries. Figure 2.2 shows this new technique. Each ternary represents a distinct class of inclusion plotted using the first three elements of the inclusion composition. Based on this method, the whole inclusion population can be observed and errors from normalizing are minimized.

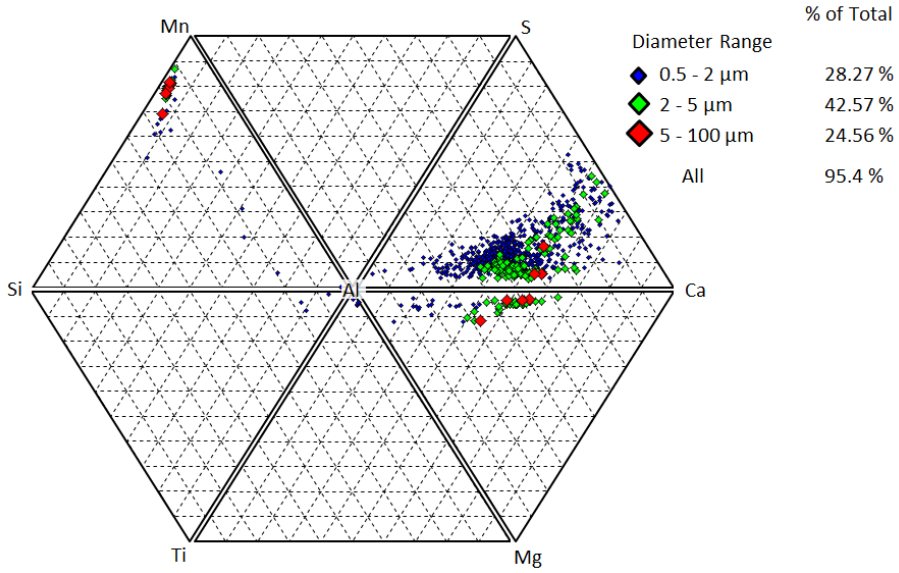

Figure 2.2 Joint ternary showing different classes of inclusions and their respective sizes where the size ranges are depicted through different colors and sizes of markers.

3. SUMMARY OF PAPERS

Paper I: An SEM/EDS Statistical Study of the Effect of Mini-Mill Practices on the Inclusion Population in Liquid Steel

Paper 1 reports on the formation and evolution of spinel during liquid steel processing of line pipe steels. Lollipop immersion samples were collected at different stages in the process and analyzed for inclusions using automated feature analysis (AFA).

From the results, spinel inclusions were observed to form after liquid steel desulfurization. This result suggests that ladle slag is the source of magnesium for spinel formation. PPM values of magnesium were also observed to be highest after desulfurization. After calcium treatment, spinel inclusions were modified to both liquid and solid calcium aluminates. Formation of CaS and MgO rich inclusions were also observed

Tundish samples showed evidence of liquid steel reoxidation and the absence of spinels after calcium treatment suggests that the observed spinel inclusions in the tundish samples formed by reoxidation. The presence of calcium sulfide inclusions (CaS) was also observed to act as a buffer to the inclusions formed by after reoxidation. Finally, comparisons were also made to different plant practices and it was observed that killing on tap produced spinel inclusions due to faster reaction kinetics.

Paper II: Characteristics of Spinel Inclusions Formed After Reoxidation of Calcium Treated Aluminum Killed Steel

Paper 2 reports on the formation of spinel inclusions after liquid steel reoxidation and also the spinel inclusion characteristics before and after reoxidation. Laboratory heats were performed in a 100Ibs vacuum induction furnace to simulate different conditions in which spinel inclusions can be formed and immersion lollipop samples collected after different stages. Analysis of inclusions was done using automated SEM/EDS. To study the inclusion size distribution, the population density function method (PDF) was applied.

Thermodynamic modeling of liquid steel reoxidation showed the possibility of spinels formation after reoxidation. Results from experimental heats showed that after

liquid steel reoxidation, pure spinel inclusions are formed if there is sufficient magnesium in solution (about 4ppm). With less magnesium, complex calcium aluminate and spinel inclusions were observed. The application of PDF to samples taken from the laboratory heats showed that spinel inclusions observed after reoxidation are larger than those observed before reoxidation.

.

PAPER

I. AN SEM/EDS STATISTICAL STUDY OF THE EFFECT OF MINI-MILL PRACTICES ON THE INCLUSION POPULATION IN LIQUID STEEL

Obinna Adaba, Marc Harris, Ronald J. O'Malley, Simon N. Lekakh, Von L. Richards

Missouri University of Science and Technology
Materials Science & Engineering Dept.
1400 N Bishop
Rolla, MO 65409

Neil Sutcliffe
Nucor Steel Gallatin
4831 US Highway 42 West
Ghent, KY 41045

ABSTRACT

The use of joint ternaries with size and color coding provides a concise means of interpreting the large quantity of data from automated feature analysis (AFA) and observing the inclusion population at different stages of steelmaking. A method was developed and applied to study the effect of mill practice such as tap practice; live vs kill-on-tap, desulfurization method, heat sequence number, and liquid steel transfer on the inclusion population. Samples for analysis were collected from two industrial steel mills. Results show the formation of spinel inclusions with long holding times in the ladle and also killing-on-tap. After calcium treatment, spinel inclusions were partly and fully modified. Also observed was the formation of CaS and MgO rich inclusions. Analysis of tundish samples showed evidence of reoxidation and also the ability of CaS inclusions to act as a buffer for reoxidation inclusions.

INTRODUCTION

Non-metallic inclusions in aluminum killed steel are often classified according to their composition, size, amount, and distribution [1-14]. The inclusion population can be composed of simple oxide inclusions such as alumina or more complex calcium aluminates with varying amounts of sulfides. Depending on the characteristics of the inclusions, they can affect the casting process by clogging submerged entry nozzles (SEN) and reduce the strength and toughness of the final product.

Many of the inclusions found in aluminum killed steel are formed during deoxidation [1,2] and a large number of studies have been devoted to the control and minimization of harmful inclusions in liquid steel [2,7]. These methods of control include the use of a lime rich, viscous, MgO saturated slag at the LMF, the optimization of argon stirring via porous plugs, calcium treatment to modify inclusions, and minimization of reoxidation during transfer through the use of refractory shrouds with argon protection at the joints. The employment of these techniques, and others, has made it possible to produce high quality steel with reduced inclusion content.

The specific melt shop practice for the production of clean steel is usually based on experience and varies from shop to shop. This paper highlights the effect of the different steelmaking practices on the inclusion characteristics during liquid steel processing. These experiments were carried out in two industrial facilities and at the Peaslee Steel Manufacturing Research Center (PSMRC), Missouri University of Science and Technology using an Aspex Pica 1020 SEM with EDS capability. To visualize and understand the inclusion characteristics at each stage of the process, a multiple ternary visualization system that incorporates information about the size distribution and the principal chemical make-up of the inclusions has been developed and applied.

EXPERIMENT PROCEDURE

Sample Collection and Preparation

Sampling was done at two industrial mills (mill A and mill C) using submerged lollipop samplers. Both mills produce steel coils via an EAF processing route. Figure 1 is a schematic of the steelmaking process for both mills. Desulfurization was achieved using a low oxygen lime rich slag and stirring with argon. Tables 1 and 2 show the sampling locations at both mills. Samples were collected, sectioned and mounted for inclusion analysis in the sub-surface region of the lollipop. This region was chosen to minimize the presence of inclusions formed during solidification and slow cooling at the interior of the sample. The sample surfaces were ground using SiC and polished to a 0.1μm finish using diamond paste. Metallographic preparation was done in accordance to ASTM E3-11 for all samples.

SEM/EDS Analysis

The Aspex Pica 1020 SEM with EDS capability was used for inclusion analysis. Scans were done at an accelerating voltage of 20 keV, and a nominal EDS detection time of 1 second. Iron was not included in the EDS analysis due to the high interaction volume in the EDS analysis and its effect on composition normalization of the inclusion. Inclusions scans were performed using a step size of 0.42μm at a magnification of 750X. For all samples, a total scan area of 30mm^2 was considered

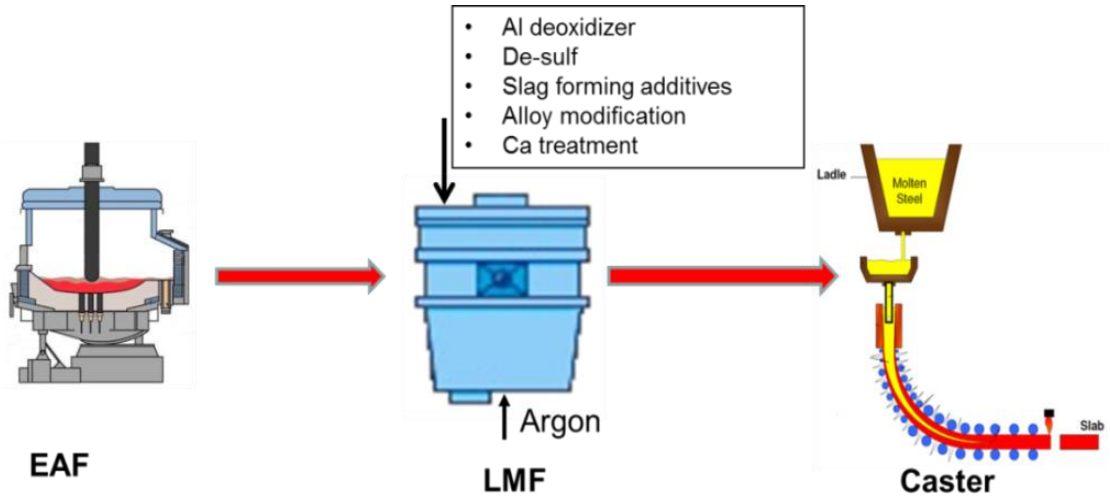

Figure 1. Steelmaking process for Mills A and C

Table1. Mill C Sample Locations

Sample No.	Steel Treatment	Stage
1	After deoxidation	LMF
2	Before desulfurization	
3	After first desulfurization	
4	After second desulfurization	
5	Before Ca addition	
6	After Ca addition	
7	94% steel remaining in ladle	Tundish
8	75% steel remaining in ladle	
9	50% steel remaining in ladle	
10	12% steel remaining in ladle	

Table 2. Mill A Sample Locations

Sample No.	Steel Treatment	Stage
1	After deoxidation	LMF
2	After desulfurization	
3	Before Ca addition	
5	After Ca addition	
6	67% steel remaining in ladle	Tundish
7	50% steel remaining in ladle	
8	33% steel remaining in ladle	

Joint Ternary with Color Codes

Inclusion compositions analyzed by the AFA method are typically represented using simple ternary diagrams, with all inclusion compositions normalized and plotted on individual ternary plots. The problem with this representation is that inclusion populations typically contain more than three elements (often 6 or 7 depending on the composition of the liquid steel). Normalization of the less abundant elements in the inclusion on a simple ternary plot can lead to misleading interpretations of the inclusion population's chemistry. Therefore, a system was developed for representing different inclusion classes based on composition [15]. The method employed here uses six different ternaries that are combined into one diagram, allowing for the representation of up to 7 elements simultaneously. Each ternary section represents a distinct inclusion population and each inclusion is only plotted in the respective ternary section that represents the three largest elements that make up the inclusion, excluding oxygen. The technique considers the three most abundant elements of a particular inclusion in assigning ternary sections and these elements typically account for more than 80% of the inclusion composition, thus errors associated with normalization are greatly reduced. In addition to minimizing normalization errors, ternaries seldom have morphological factors such as size included, which can make interpretation misleading (e.g. large exogenous inclusions of differing composition are not easily recognized). Therefore, inclusion diameter is also represented in the joint ternaries developed in this study and displayed using different colors and marker sizes.

RESULTS AND DISCUSSION

Inclusion Evolution (Mill C)

Figure 2 shows the number density and area fraction of inclusions for samples taken at mill C. From this figure, we observe a decrease in the number density and coarsening of inclusions prior to calcium treatment. This suggests that inclusions are formed at the initial stages of LMF and that there is simultaneous growth and flotation with LMF time. After calcium treatment, there is an increase in both the number density and area fraction of inclusions due to formation of new inclusions. Figure 3 shows the composition of the samples at the different stages. Samples shown are for the second heat of a cast sequence. After deoxidation with aluminum, alumina inclusions are formed. However, the presence of some calcium in the inclusions at this stage of processing indicates a calcium source. Calcium pickup may occur from slag entrainment during mixing or from calcium present in alloy additions. With time, the inclusions increase in size. After deoxidation and desulfurization, the inclusions are slowly transformed to partly modified spinels. The transformation to spinel is in agreement with current literature that suggests that MgO in slag is a likely source of magnesium pickup in steel during steelmaking [1,4,6]. As a result of the interaction between the steel and slag, MgO in slag is reduced by aluminum according to equation 1. This reaction produces dissolved magnesium in steel which further reacts with alumina to form spinel. This reaction proceeds according to equation 2. After calcium treatment, some inclusions are partly modified to liquid calcium aluminate while others are fully modified. CaS and MgO rich inclusions are also formed. The presence of CaS inclusions suggests excessive calcium treatment. These inclusions are detrimental to the casting process and should be minimized. An analysis of tundish inclusions shows similar types of inclusions to those observed after calcium treatment. However, the presence of fine (<2μm) size alumina and spinel inclusions are also observed in the tundish samples, suggesting reoxidation.

$$(MgO) + [Al] = Al_2O_3 + [Mg] \quad (1)$$

$$[Mg] + [O] + (Al_2O_3) = MgO{\cdot}Al_2O_3 \quad (2)$$

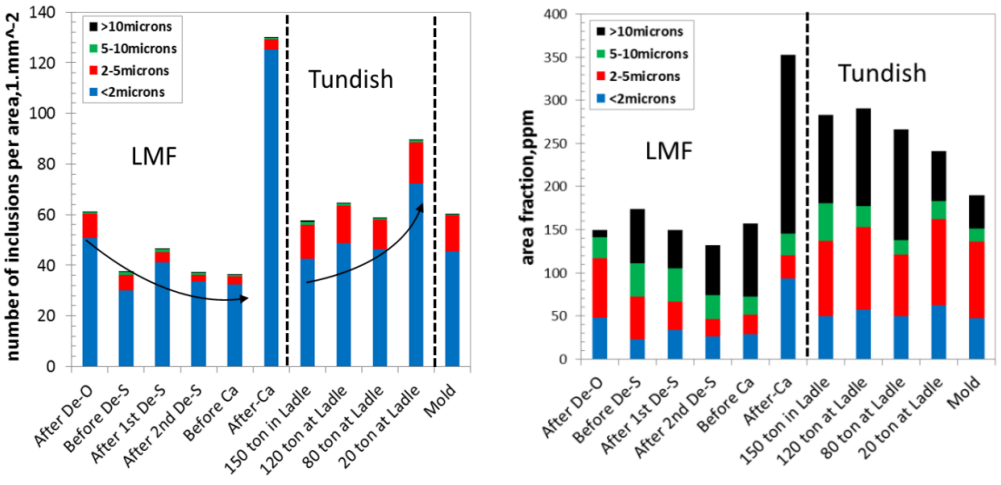

(a) (b)

Figure 2. Change in inclusion population density at different stages. (a) number density, (b) area fraction. Figure shows nucleation after deoxidation and simultaneous growth and flotation with time.

Inclusion Evolution in Ladle (Mill A)

Figure 4 shows the composition of inclusions in mill A after deoxidation, desulfurization, and calcium treatment. Spinel inclusions are also observed after a holding time in the ladle following killing and desulfurization. After calcium treatment, both partially and fully modified inclusions as well as CaS and MgO rich inclusions are observed as well. The difference in the inclusion population at mills A and C is the absence of calcium in the inclusions after deoxidation at mill A. As mentioned earlier, the presence of calcium in the inclusions observed in mill C may be due to calcium containing alloying additions or more intense stirring conditions causing slag entrainment.

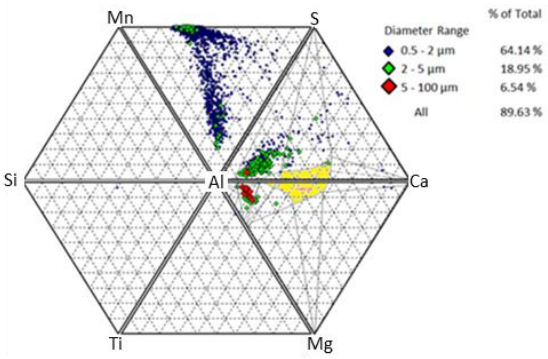

(a) After deoxidation

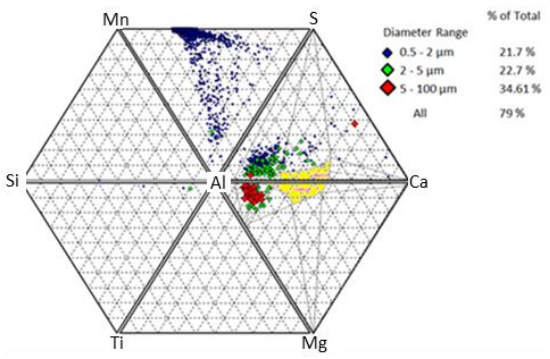

(b) Before desulfurization

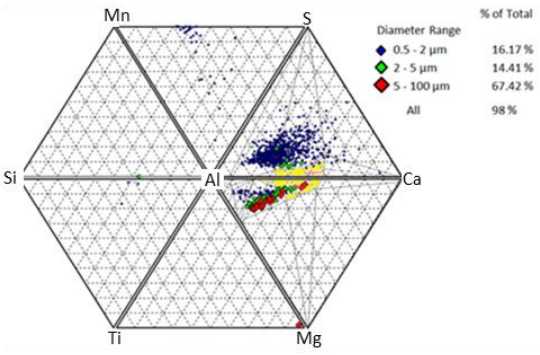

(c) Before calcium treatment

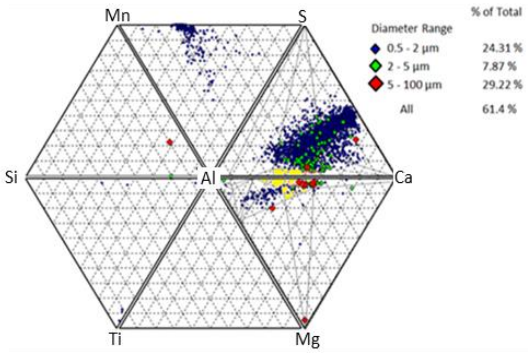

(d) After calcium treatment

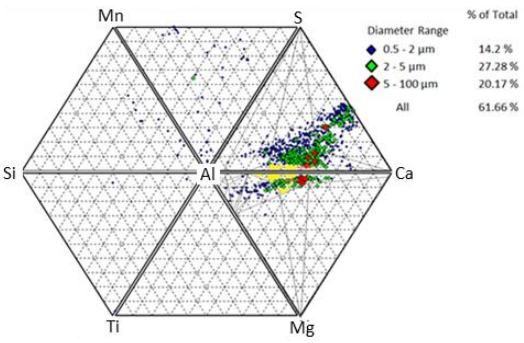

(e) Tundish (80 ton in ladle)

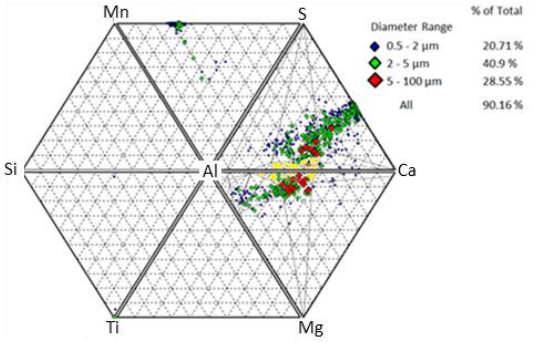

(f) Coil (center of third slab)

Figure 3. Inclusion evolution in mill C. Spinel inclusions formed after desulfurization, suggesting slag as the source of magnesium. After Ca treatment, some inclusions are partially modified and some are fully modified. CaS and MgO rich inclusions also observed.

Note: The yellow regions denote the target liquid phase fields in the $CaO\text{-}Al_2O_3\text{-}MgO$ and $CaO\text{-}Al_2O_3\text{-}CaS$ ternary systems at 1600 C. The tie lines for these systems are also shown.

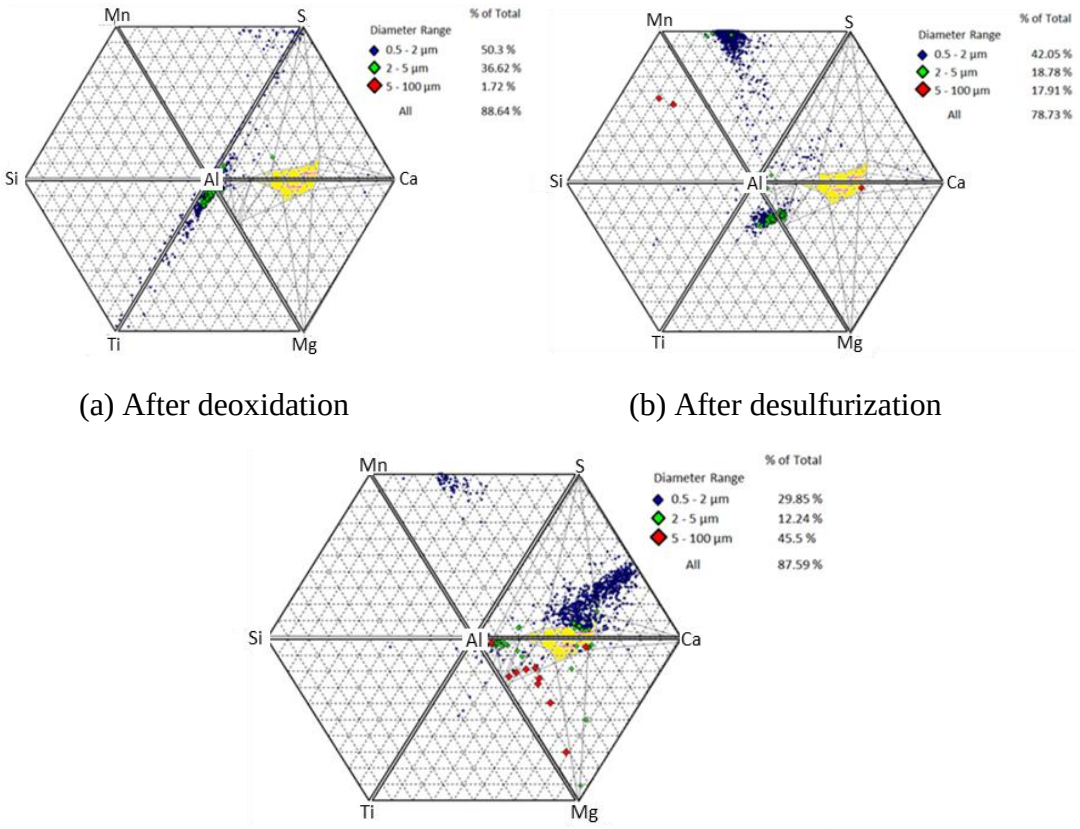

(a) After deoxidation

(b) After desulfurization

(c) After calcium treatment

Figure 4. Mill A inclusion composition, (a) after deoxidation (b) after desulfurization, and (c) after calcium treatment. Figure shows the formation of spinel with holding time in the ladle and the formation of partly and fully modified spinel inclusions, CaS, and MgO rich inclusions.

Inclusion Evolution during Tundish Transfer.

From Figure 2, it can be seen that the number of small sized inclusions (<2µm) increased during transfer from ladle to tundish. This implies occurrence of reoxidation during transfer. Figure 5 shows the change in composition of the inclusions during transfer. At the start of transfer (Figure 5a), oxide inclusions are both fully and partly modified and CaS inclusions are also present. However, with continued transfer from ladle to the tundish (Figure 5b-c), newly formed fine alumina and spinel inclusions which are less than 2µm in size are observed. The formation of these inclusions is due to the reaction of dissolved aluminum in the steel with oxygen according to equation 3. This reoxidation also produces MnS inclusions (Figure 5d) through the oxidation of CaS. These MnS

inclusions are not actually present in the liquid steel, but instead form during solidification of the steel sample [5]. During reoxidation, CaS inclusions can be oxidized and sulfur returned to steel, reappearing as MnS in in the steel sample. Equations 4 and 5 show the reaction sequence. The observed trend in Figure 5 also suggests that CaS inclusions can acts as a calcium buffer for inclusion modification during reoxidation.

$$2[Al] + 3[O] = (Al_2O_3) \quad (3)$$

$$(CaS) + [O] = (CaO) + [S] \quad (4)$$

$$(CaO) + (Al_2O_3) = (CaO \bullet Al_2O_3) \quad (5)$$

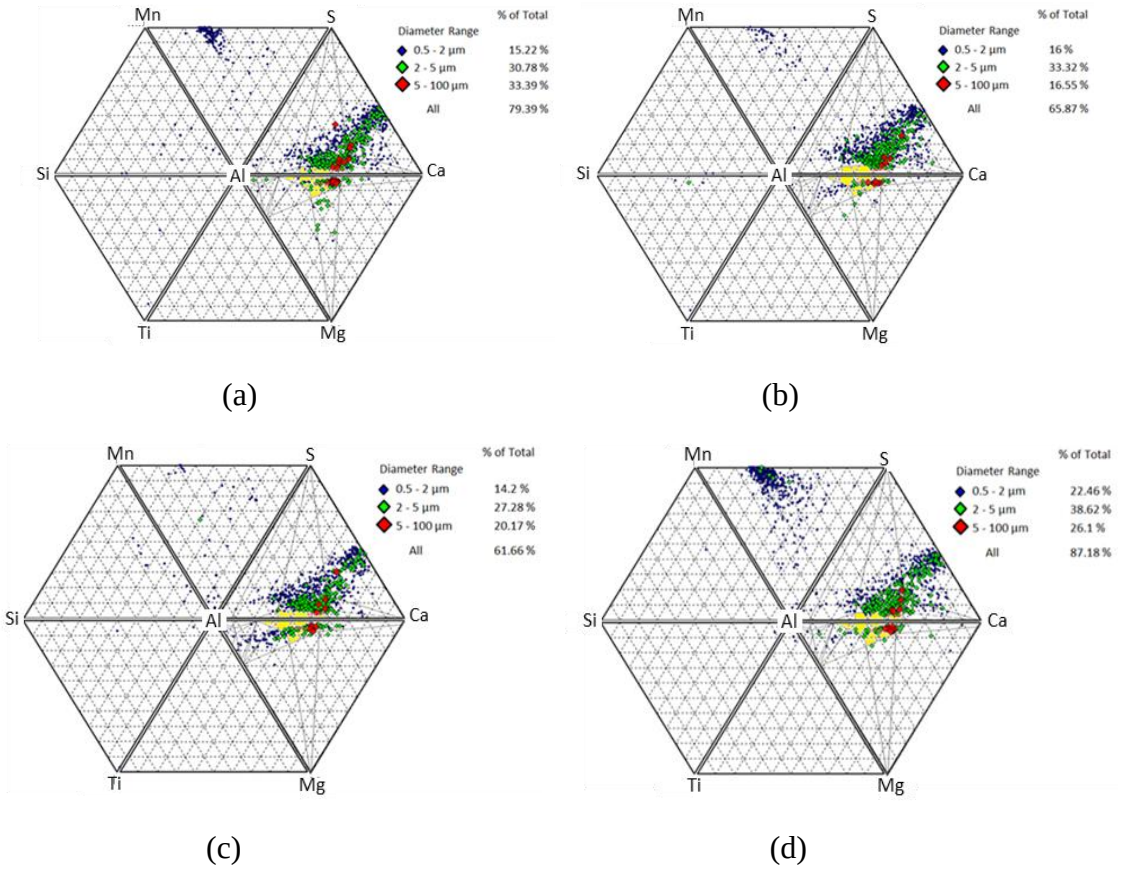

Figure 5. Mill C inclusion evolution during transfer from ladle to tundish (a) 150 ton in the ladle (b) 120 ton in the ladle, (c) 80 ton in the ladle, and (d) 20 ton in the ladle. Tundish analysis shows reoxidation during transfer. Transformation from CaS to MnS inclusions and the absence of spinel formation shows ability of CaS to buffer reoxidation inclusions.

Two specific cases:

(a) Inclusions in a Startup Heat

Lollipop samples were collected at the final stages of LMF processing and in the tundish for a startup heat in mill C. Figure 6 shows the number density and area fraction for samples collected in this heat. As can be seen, there is an increase in both the number and area of the inclusions as steel is transferred from the ladle to the tundish. As shown by the inclusion composition in Figure 7, there is an observed change in inclusion characteristics from final LMF to tundish. During the transfer, the heat is opened without any slag covering and this exposes the steel to atmospheric oxygen. We observed the formation of fine alumina inclusions during the initial stages of transfer (Figure 6a). Once the steel in the tundish reaches a sufficient height to submerge the ladle shroud, slag is then added and the remaining steel is transferred under the protection of a tundish slag. The addition of slag resulted in a decrease in the number and area fraction of inclusions. The samples also showed a decrease in the amount of fine alumina inclusions later in the heat after the tundish slag cover was added.

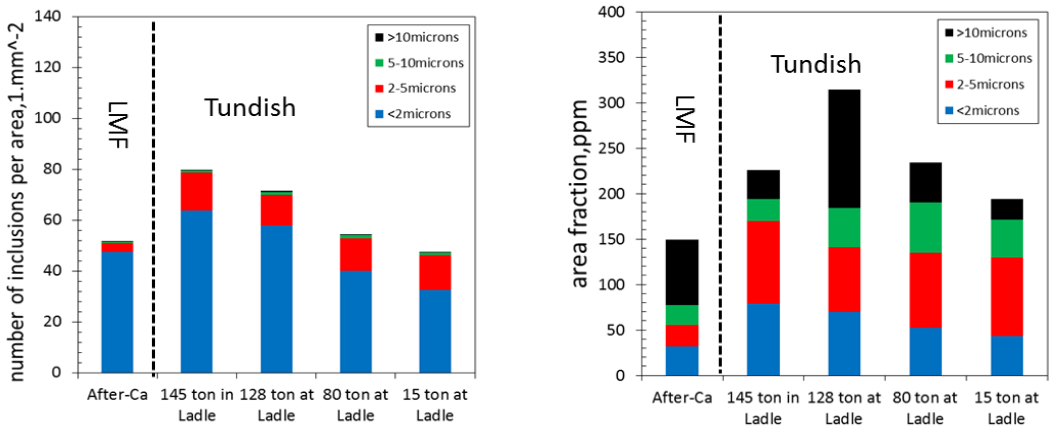

(a) (b)

Figure 6. Change in inclusion population density for a startup heat (mill C). (a) number density, and (b) area fraction. Figure shows the effect of slag addition as the number and area fraction of fine inclusions decrease with tundish transfer.

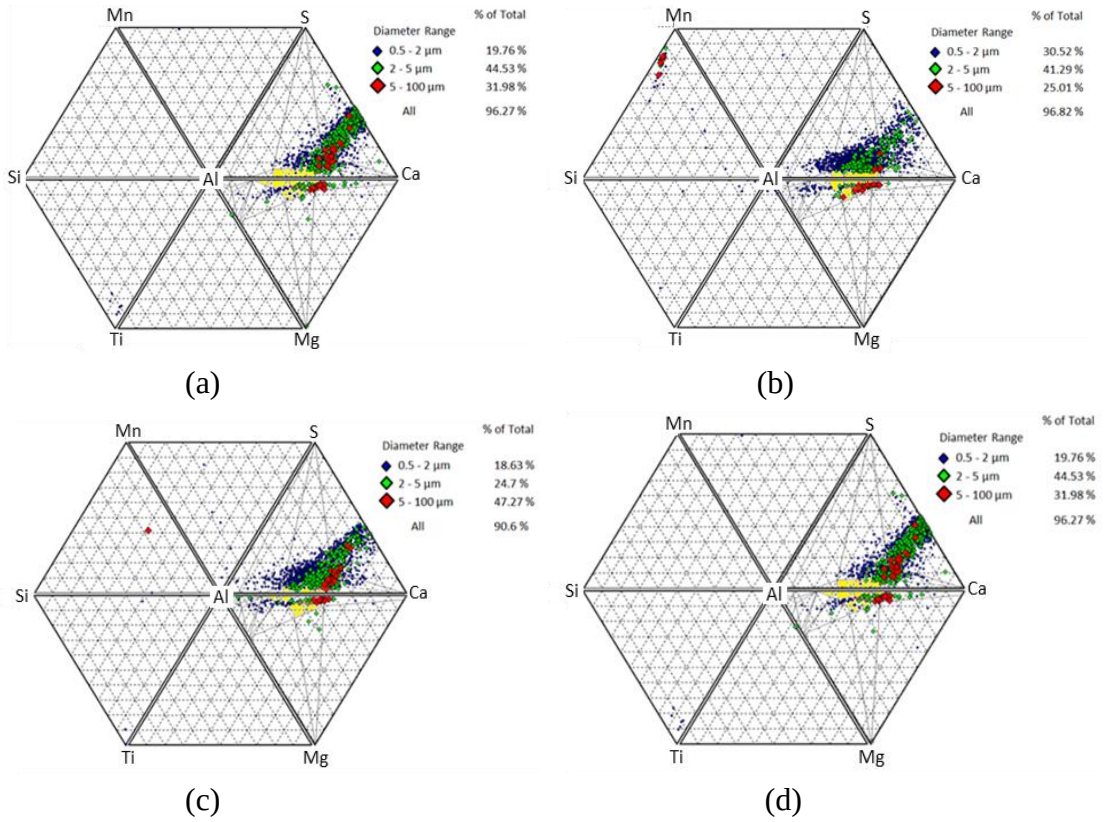

Figure 7. Inclusion evolution for startup heat (mill C). (a) final LMF (b) tundish, 145 ton in the ladle, (c) tundish, 80 ton in the ladle, and (d) tundish, 15 ton in the ladle. Alumina inclusions formed during tundish transfer decrease with time due to addition of slag.

(b) Effect of Tap Practice

The effect of EAF tap practice on the inclusion population was investigated in mill A. Two tap practices were studied; a live-tap practice and a kill-on-tap practice. In the live-tap practice, the steel from the EAF was tapped into the ladle before any aluminum was added for deoxidation. In the kill-on-tap practice, Al was added to the tap stream during EAF tapping into the ladle. Figure 8 shows the inclusion distribution for both processes. As can be seen, the inclusion population is composed predominantly of spinels using the kill-on-tap practice, whereas the inclusion population is composed predominantly of alumina using the live-tap practice. Both ladle slag and the refractory are potential sources of Mg due to their high MgO contents. With the kill-on-tap practice, the stream provides additional energy to promote the reduction of MgO by Al according to Eq.1 when the oxygen content of the steel is low. This produces a higher amount of dissolved magnesium in steel, and thus, favors the formation of spinels.

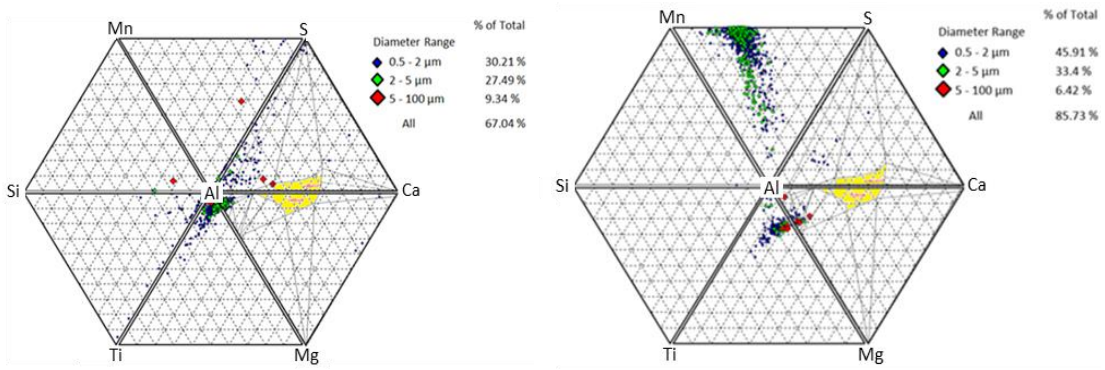

(a) (b)

Figure 8. Inclusion distribution for both EAF tap procedures. (a) live tap, (b) kill on tap. Both samples were collected at about 30 minutes after deoxidation and prior to any other additions in the ladle.

CONCLUSION

The effect of steelmaking practice on the inclusion population was studied at two industrial mills that produce coils via the EAF route. Samples were taken at different stages in the steel making process as well as from different heats in a cast sequence. AFA analysis showed that spinel inclusions formed due to interaction of steel with the slag when the oxygen level in the steel is low. After calcium treatment, the spinel inclusion population was both partly and fully modified. CaS and MgO rich inclusions also formed after Ca treatment. Tundish samples showed evidence of steel reoxidation, through the presence of newly formed fine alumina and spinel inclusions. On a startup heat, evidence of reoxidation was observed shortly after tundish fill and then decreased with time. For samples taken from the tundish in the second heat in a sequence, reoxidation was observed to increase with time.

A comparison mill practices showed that inclusions in mill C were partly calcium modified immediately after deoxidation. In contrast, the inclusions in mill A contained no calcium after deoxidation. The observed difference is believed be due to different argon stirring practices or alloying additives that contain calcium. A comparison of different EAF tap practices showed that spinel inclusions formed when steel deoxidation was performed during tapping, whereas, for the live-tap practice, alumina inclusions were formed.

ACKNOWLEDGEMENT

The authors would like to give special thanks the team at Nucor Gallatin for assisting in the industrial data and sample collection and to the industrial members of the Peaslee Steel Manufacturing Research Center (PSMRC) for their financial support of this project.

REFERENCES

1. E.B Pretorius, H.G. Oltmann and B.T. Schart "An Overview of Steel Cleanliness from an Industry Perspective", AISTech 2013: 993-1026.

2. Zhang, Lifeng, and Brian Thomas. "State of art in Evaluation and Control of steel Cleanliness", *ISIJ International* 43, (2002): 271-291.

3. N. Verma, P.C Pistorius, R.J Fruehan, M.S. Potter, H.G. Oltmann, E.B, Pretorius, "Calcium Modification of Spinel Inclusions in Aluminum-Killed Steel: Reaction Steps", *Metallurgical and Materials Transactions B* 43.4 (2012): 830-840.

4. V. Singh, S. Lekakh, T.J. Drake, K.D. Peaslee, "Process Design of Inclusion Modification in Cast Steel using Automated Inclusion Analysis", AISTech 2009.

5. H.G. Oltmann, E.B, Pretorius, "The Effective Modification of Spinel Inclusions by Ca treatment in LCAK", *Iron & Steel Technology* 7.7 (2010): 31-44.

6. Verma, Neerav, Petrus Pistorius, Richard Fruehan, Michael Potter, Minna Lind, and Scott Story. "Transient Inclusion Evolution during Modification of Alumina Inclusions by Calcium in Liquid Steel: Part I. Background, Experimental Techniques, and Analysis Methods" *Metallurgical and Materials Transactions B* 42.4 (2011): 711-719.

7. Verma, N., Petrus Pistorius, Richard Fruehan, Michael Potter, Minna Lind, and Scott Story. "Transient Inclusion Evolution During Modification of Alumina Inclusions by Calcium in Liquid Steel: Part II. Results and Discussion", *Metallurgical and Materials Transactions* B 42.4 (2011): 720-729.

8. P.Chris Pistorius, Peter Presoly, and K. Ghislain Tshilombo. "Magnesium: Origin and role in Calcium-Treated Inclusions", *SOHN International Symposium on Advanced Processing of Metals and Materials: Principles, Technologies and Industrial Practice*, San Diego, California, 27-31 August 2006: 373-378.

9. Deng, Zhiyin and Miaoyong Zhu. "Evolution Mechanism of Non-metallic Inclusions in Al-Killed Alloyed Steel during Secondary Refining Process" *ISIJ International* Vol. 53, No. 3 (2013): 450-458.

10. Abraham, Sunday, Justin Raines, and Rick Bodnar. "Development of an Inclusion Characterization Methodology for Improving Steel Product Cleanliness", *AIST Transactions*, Vol. 11, No. 2 (2013): 1069-1083.

11. Kaushik, P., H. Pielet, and H. Yin. "Inclusion Characterization – Tool for Measurement of Steel Cleanliness and process control: Part 1." *Ironmaking and Steelmaking* 36: 561-571.

12. Kaushik, P., H. Pielet, and H. Yin. "Inclusion characterization – tool for measurement of steel cleanliness and process control: Part 2." *Ironmaking and Steelmaking* 36: 572-582

13. Higuchi, Yoshihiko, Mitsuhiro Numata, Shin Fukagawa, and Kaoru Shinme. "Inclusion Modification by Calcium Treatment." *ISIJ Int.* 36: 151-154.

14. Yang, Wen, Lifeng Zhang, Xinhua Wang, Ying Ren, Xuefeng Liu, and Qinglin Shan. "Characteristics of Inclusions in Low Carbon Al-Killed Steel during Ladle Furnace Refining and Calcium Treatment", *ISIJ Int.* 53, (2013): 1401-1410.

15. "Improved Methodology for Automated SEM/EDS Non-Metallic Inclusion Analysis of Mini-Mill and Foundry Steels", M. Harris, O. Adaba, S. Lekakh, R. O'Malley, and V. L. Richards, Proc. AISTech 2015, Cleveland, May 4-7, 2015, pp. 2315-2325.

II.CHARACTERISTICS OF SPINEL INCLUSIONS FORMED AFTER REOXIDATION OF CALCIUM TREATED ALUMINUM KILLED STEEL

Obinna Adaba[1], Pallava Kaushik [2], Ronald J. O'Malley[1], Simon N. Lekakh[1], Erik Mantel[2], Randy Hall[2], Eric J.Ellis[2].

[1]Missouri University of Science and Technology
Materials Science & Engineering Dept.
1400 N Bishop
Rolla, MO 65409

[2]ArcelorMittal Global R&D
3001 East Columbus Drive
East Chicago, IN-46530

ABSTRACT

Reoxidation of liquid steel during the last stages of production affect the inclusion characteristics and is harmful to process stability, mechanical properties, and the overall quality of the cast product. A laboratory vacuum induction furnace was employed to simulate the reoxidation of aluminum killed calcium treated steel to observe the formation of spinels. Immersion samples were collected at different times in a laboratory and analyzed via automated SEM/EDS. A method for representing the size distribution of inclusions using the population density function (PDF), was applied to study the effect of reoxidation on the change in size of spinel inclusions. The results show that spinel inclusions can be produced after reoxidation if there is sufficient magnesium in solution. A comparison of the size distributions of spinel inclusion populations showed that spinel inclusions formed after reoxidation are larger than those formed prior to reoxidation and calcium treatment.

INTRODUCTION

Reoxidation of liquid steel during the last stages of steel production affects the inclusion characteristics and is harmful to process stability, mechanical properties, and the overall quality of the cast product [13]. For aluminum killed steel, alumina inclusions generated after deoxidation clog submerged entry nozzles (SEN) and their irregular shape acts as sites for crack initiation. To avoid this, calcium is typically used at the end of LMF to modify the solid alumina inclusions to liquid spherical calcium aluminates. Liquid steel reoxidation leads to the formation of new alumina inclusions which in the absence of calcium, retain their inclusion characteristics and spoils the benefit of calcium treatment. In steels with sufficient magnesium in solution, spinel inclusions can also be formed after reoxidation [12,13]. These inclusions have been observed to cause hook cracks in line pipe steels and thus, rejection and loss of resources [9].

Formation of Spinels in Ca-Treated Reoxidized Steel

Results from studies conducted at an industrial mini mill showed ladle slag as the source of magnesium in liquid steel [8]. Spinel inclusions were observed after the desulfurization process where the steel was continuously mixed with the MgO saturated slag using argon gas. Eq. 1 and Eq. 2 describe the two step mechanism for the formation of spinels.

$$3(MgO) + 2[Al] = 3[Mg] + (Al_2O_3) \quad (1)$$

$$[Mg] + 2[Al] + 4[O] = (MgO \cdot Al_2O_3) \quad (2)$$

At the end of ladle metallurgy processing, these inclusions were modified by calcium to liquid calcium aluminates. These modified inclusions are less harmful to the casting process and steel properties. Also observed was the formation of CaS inclusions that resulted from over treatment. The reaction mechanism for the calcium modification of spinels is given by eq. 3 and shows the possibility of magnesium re-dissolution into steel.

$$[Ca] + (MgAl_2O_4) = CaO \cdot Al_2O_3 + [Mg] \quad (3)$$

Thermodynamic calculations using commercial software, allow for consideration of complex reactions involving the formation of oxide and sulfide inclusions. In such simulations, several assumptions can be made. For example, calculations can be done with additions into a closed system, or into a partially open system by removing selected reaction products. Calculations were done using Factsage 6.4 to simulate both the calcium modification process, and the effect of liquid steel reoxidation on the change in the inclusion. These calculations were done at a temperature and pressure of 1600 ˚C and 1atm. respectively using a typical line pipe steel composition. Figure 1a shows the results of the calcium modification process in a closed liquid steel system. Optimum calcium content of 10-20 ppm, results in fully modified spinel inclusions. At higher levels of calcium, solid CaS inclusions are formed. During this process, the dissolved magnesium content in the liquid steel is increased from less than 1ppm to about 4ppm (fig 1b) as the spinel inclusions are modified to liquid calcium magnesium aluminate inclusions. This calculation was done for an alumina saturated spinel (80% $Al_2O_3$and 20% MgO). Also shown in figure 1b is the calculated increase in dissolved magnesium during modification

of MgO saturated spinel inclusion. At steelmaking temperatures, single phase spinel is stable over a range of MgO contents. The MgO content varies from 20-30%. For an MgO saturated spinel, the amount of dissolved magnesium in steel is seen to be as high as 12ppm.

Reoxidation of Ca-treated liquid steel during steel transfer from the ladle and into tundish and mold has been observed in industrial practice and spoils the benefits of the calcium treatment. To study the effect of reoxidation on the inclusions, thermodynamic calculations were done for initial 21ppm calcium treated steel with different amounts of added oxygen. The result of this calculation is shown in figure 2. After reoxidation with 30ppm oxygen, newly formed spinel and solid calcium aluminate inclusions are observed in the liquid steel. With increased oxygen content, these inclusions transform to more complex solid calcium magnesium aluminates. These results from both thermodynamic calculations clearly indicate that:

1. Calcium reacts with MgO in spinel and in conditions where Mg vaporization is suppressed, magnesium dissolves in liquid steel. This is in agreement with literature [8,12].

2. Liquid steel reoxidation after calcium treatment can produce newly formed spinel inclusions when there is sufficient magnesium in solution.

To verify these results and also to compare the spinel inclusion size and shape formed after reoxidation, with those observed before reoxidation, laboratory experiments were carried out to investigate calcium treatment and reoxidation of liquid steel. To represent the size distribution of the inclusions, the method of population density function (PDF) was applied.

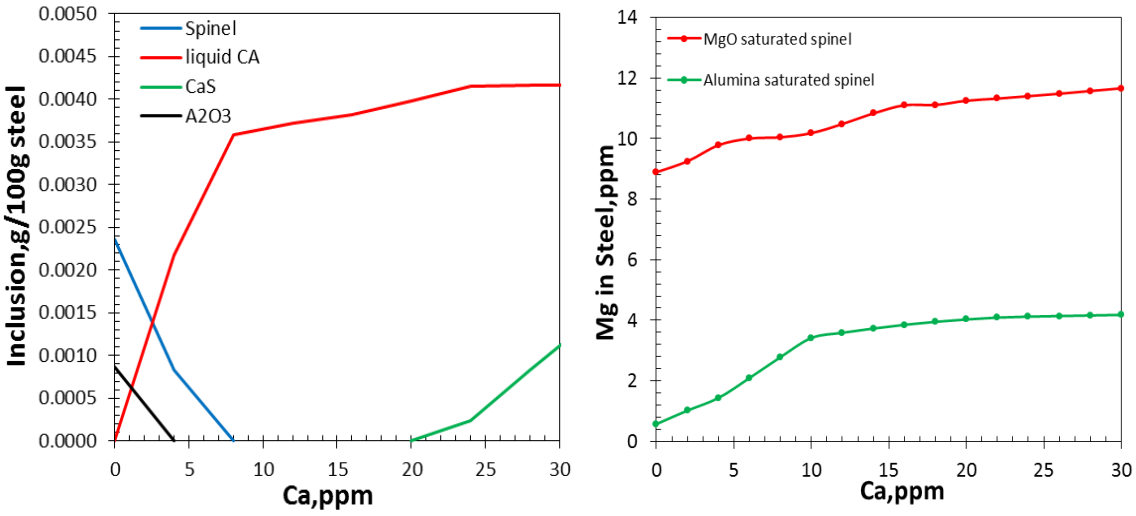

(a) (b)

Figure 1: Thermodynamic simulation of spinel modification by calcium using Factsage 6.4. Target liquid inclusions form between 10 to 20 ppm Ca. Dissolved magnesium also increases during the process.

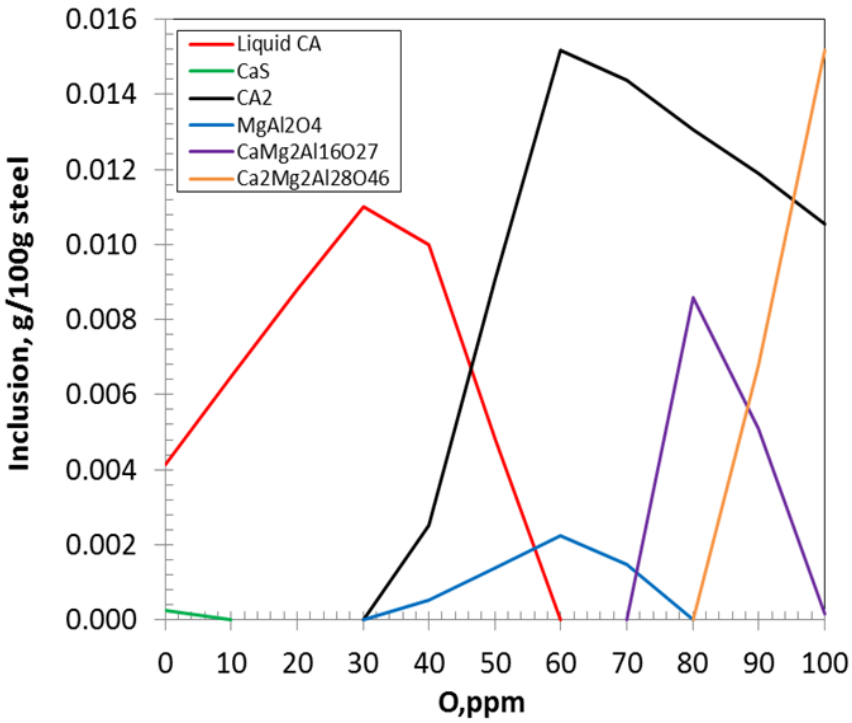

Figure 2: Thermodynamic simulation of the inclusion evolution in reoxidized calcium treated steel. Newly formed spinel inclusions are observed in steel reoxidized with 30ppm oxygen.

Size Distribution of Inclusions

Reoxidation of liquid steel produces new inclusions and can be observed from the change in shape of the inclusion size distribution [1]. The size distribution of non-metallic inclusions can be described by either log-normal or fractal distributions depending on the chemical and physical processes occurring in the liquid steel [1,3,4]. These distributions are described by eqs.4 and 5 respectively. Where f(x) is the frequency of inclusions in a given size bin or population density function (PDF), and "x" is the inclusion diameter. "α" and "β" are constants related to the mean and shape of the log normal distribution, and "C" and "D" are constants of the fractal distribution. In a ln-ln plot of the PDF and inclusions diameter, the shape of the PDF is either quadratic or linear [1,2]. This is shown by eqs.6 and 7 respectively.

$$f(x) = \left[\frac{1}{x\beta\sqrt{2\pi}}\right]\exp\left[-\left(\frac{1}{2\beta^2}\right)(lnx - \alpha)^2\right] \quad (4)$$

$$f(x) = \frac{C}{x^D} \quad (5)$$

$$\ln(f(x)) = \frac{-(lnx)^2}{2\beta^2} + \left(\frac{\alpha-\beta^2}{\beta^2}\right)(lnx) + \ln\left(\frac{1}{\beta\sqrt{2\pi}}\right) - \frac{1}{2\beta^2}\alpha^2 \quad (6)$$

$$\ln(f(x)) = \ln(C) - D\ln(x) \quad (7)$$

Different methods have been applied to interpret the size distribution of particles [4]. The concept of population balance was first introduced and developed by Randolph and Larson in the field of chemical engineering [2,3] and later applied to rocks by Marsh [2] . This method is based on population balance of number of particles in a given size range. By making assumptions of continuous nucleation and size independent growth rate for crystal rocks, a plot of the log of the frequency and size produced a linear distribution. Cashman et al [1], however, also observed quadratic distributions in some systems and proposed Ostwald ripening as the cause for the shape change. Figure 3 shows the proposed mechanism for the different shape distributions by Cashman.

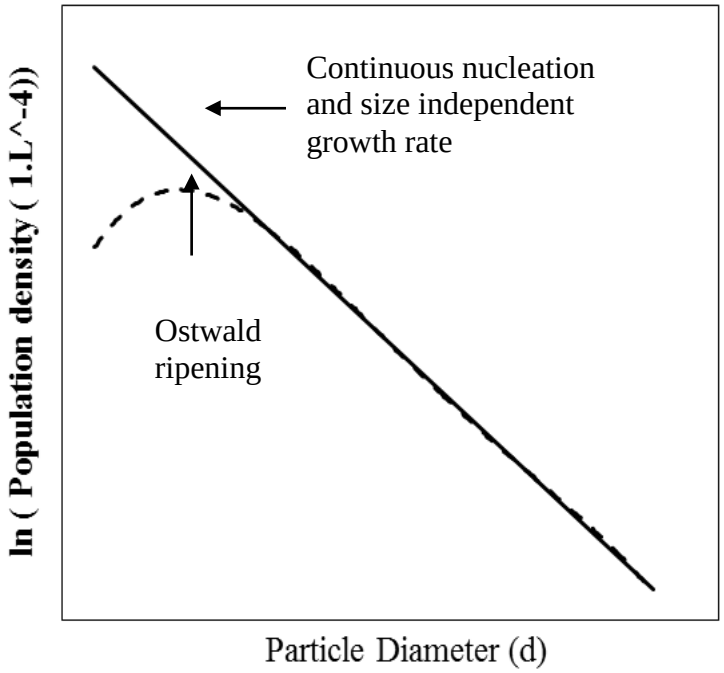

Figure 3: Particle distributions and the mechanism of formation. Mechanism proposed by Marsh. Distribution starts as linear and transforms to quadratic shape due to Ostwald ripening.

Due to failure of population balance technique to successfully model the particle shape for many crystal systems in nature and from observations that most crystal size distributions are lognormal, Eberl et al [4], simulated the growth of crystals under different conditions by numerical methods. Based on values of 'β' and 'α', growth mechanisms for different crystal size distribution (CSD) shapes were proposed. Table 1 is a summary of the proposed growth mechanisms under different conditions. This method of describing the size distribution of particless using PDF was applied to non-metallic inclusions by E. Zinngrebe et al [1] and from their studies, lognormal distributions observed after aluminum deoxidation transformed to linear at the end of the LMF. They proposed this linear distribution to result from conditions of kinetic equilibrium between the liquid steel and inclusions.

The PDF method was applied to lollipop samples taken during a startup heat to observe the conditions which produce each shape distribution. The samples were taken from an industrial mini mill during liquid steel processing and are different from the laboratory samples. For a startup heat, reoxidation has been observed to occur during liquid steel

transfer from the ladle to the tundish. This is because the liquid steel is totally exposed to the atmosphere at the start of transfer until a sufficient amount of steel has been tapped into the tundish and after which slag additions are made.

.

Table 1: Proposed growth mechanisms for different CSD shapes [4].

System	Growth Mechanism	CSD Shape	Comments
Open	Nucleation and growth with constant or accelerating nucleation rate.	Asymptotic.	β^2 increases exponentially with increase in α.
	Nucleation and growth with decaying nucleation rate.	Lognormal.	β^2 increases linearly with increase in α.
	Surface-controlled growth.	Lognormal.	β^2 increases linearly with increase in α.
	Supply-controlled growth.	Preserves shape of previous CSD.	β^2 remains constant with increase in α; therefore, steady-state reduced profiles.
Closed	Ostwald ripening (supply-controlled).	CSD becomes more symmetrical with increasing percentage of ripening, becomes negatively skewed, and eventually approaches universal steady-state reduced profile.	Distribution maximum moves to the right of theoretical lognormal curve. Generally, β^2 decreases with increase in α. Universal steady-state profile may not be reached.
	Random ripening (supply-controlled). Also termed non-Ostwald or kinetic ripening.	Preserves shape of previous CSD.	A large amount of material passes through solution for a small increase in mean size. β^2 remains constant with increase in α; therefore steady-state reduced profiles.
	Agglomeration.	Can be pseudo-lognormal or multimodal, or have other shapes.	Very little material need pass through solution for a large increase in mean size. If most of the crystals are involved, β^2 may decrease; otherwise it may increase.

RESULTS AND DISCUSSIONS

Laboratory Experiment and Sample Analysis

To verify the formation of spinels after reoxidation, laboratory experiments were carried out in a 100lbs vacuum induction furnace. Three heats with changes in the alloy and time of additions after calcium treatments were performed. Figure 4 is a schematic of the three heats and the respective additions. After melting and before alloy additions, air was removed and the chamber filled with argon gas to 0.7atm. Oxygen was added in the form of Fe_2O_3 while magnesium and calcium were added in the form of magnesium alloy and

calcium silicon wire (CaSi) respectively. Immersion lollipop samples were taken after respective additions.

Collected lollipop samples were analyzed for liquid steel composition and inclusions. To determine the magnesium content, induction coupled plasma (ICP) was used while spark emission spectrometer was used for other elements. After chemical analysis, samples were section, polished, and analyzed for inclusions using automated SEM/EDS. A scan area of 100mm^2 was considered for all samples and the minimum inclusion size detected was 1μm.

Formation of Spinel after Reoxidation

Figure 5 shows the inclusion evolution for heat 1 after each alloy addition. After aluminum deoxidation, the inclusion population consisted of alumina inclusions and transformed to both spinel and MgO inclusions after the addition of magnesium. Calcium modified the spinels to both solid and liquid calcium aluminates and CaS inclusions were also produced. The absence of pure MgO inclusions after calcium addition suggests that sample 2 was taken when the inclusions were at a transient stage.

50ppm oxygen was added for reoxidation after calcium treatment. The addition of oxygen shifted the inclusion population towards the alumina rich region and the population consisted of complex calcium aluminate and spinel inclusions. Pure spinel inclusions were not observed. Based on the proposed reaction mechanism for the calcium modification of spinel, magnesium goes into solution after reoxidation. The lack of pure spinels suggests that there might not have been enough magnesium in solution. Chemical analysis showed a consistent Mg analysis of less than 3ppm in samples 2, 3, and 4. Dissolved Mg however, can be as low as 0.5ppm. To measure the small amounts of Mg, a change was made to the standard for ICP and applied to heats 2 and 3.

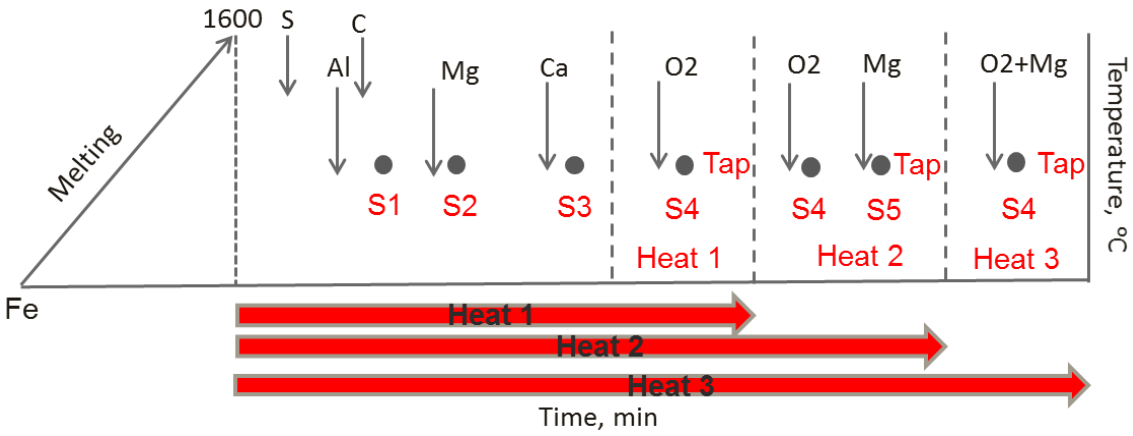

Figure 4: Schematic of the three heats and the respective alloying and sampling positions.

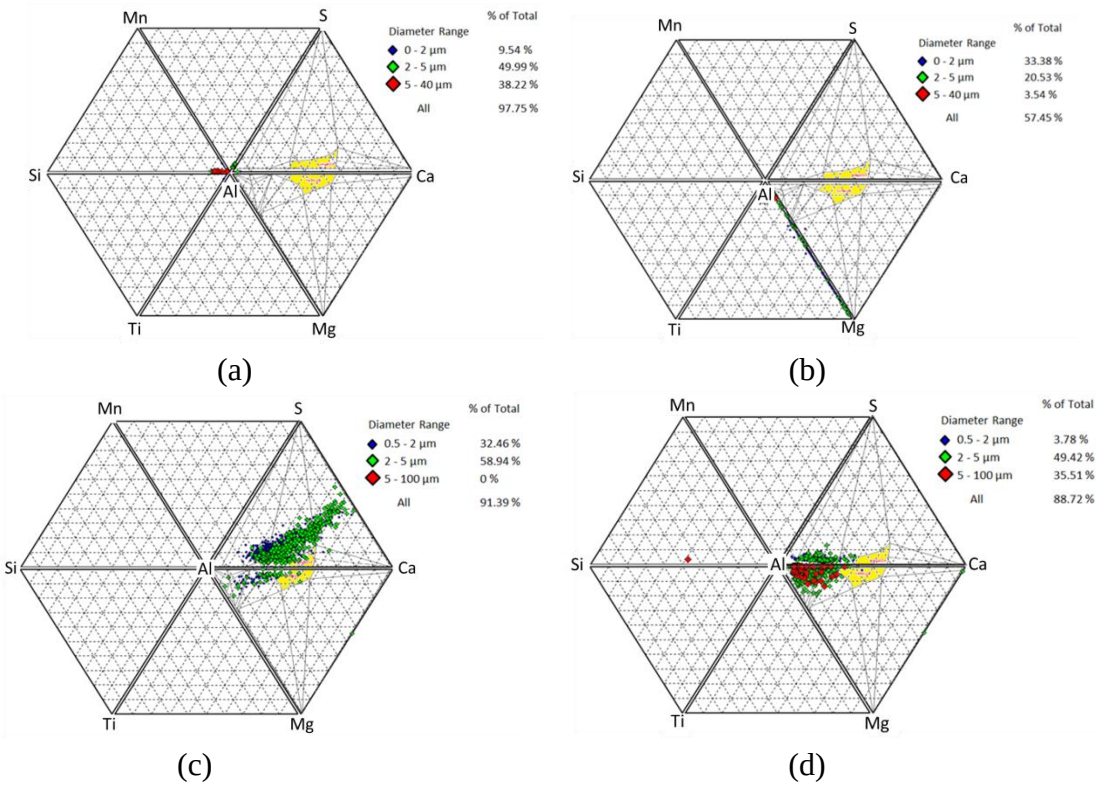

Figure 5: inclusion evolution for heat 1. (a) after deoxidation, (b) after addition of magnesium, (c) after calcium treatment, (d) After reoxidation.

For heats 2 and 3, the added CaSi wire was increased from 200g to 250 g. Also, 80g NiMg was added after calcium treatment and reoxidation to produce spinel inclusions. For heat 2, the magnesium was added after the addition of oxygen while in heat 3 both magnesium and oxygen where added at the same time. Tables 2 and 3 show the steel

composition of the samples collected in both heats. Both heats showed the magnesium content before calcium treatment to be about 2ppm. After calcium treatment, no change in magnesium was observed and suggests that magnesium dissolved in solution.

After the addition of NiMg, the total magnesium increased by about 3 ppm. Based on mass balance calculations 80g NiMg should have produced an increase of about 15ppm Mg. The result therefore suggests that most of the magnesium vaporized on addition and went to the atmosphere. Figures 6 and 7 show the inclusion composition for samples in both heats taken after the addition of calcium and also after reoxidation and addition of magnesium. After reoxidation and addition of magnesium, pure spinel and MgO inclusions are observed in both heats. The simultaneous addition of both magnesium and oxygen however, produced more spinel and also liquid calcium aluminate inclusions. This result suggests that there was both reduction and dissolution occurring at the same time. Both results suggest that if there is sufficient magnesium (about 4ppm) in solution after calcium treatment, and reoxidation occurs, pure spinel inclusions will be formed.

Table 2: Composition of Samples (Heat 2)

Time, min	Sample No.	Composition, wt.%				
		C	Al	S	Ca	Mg
0	Sample 1- after Al	0.041	0.08	0.006	0.0001	0.00008
5	Sample 2- after NiMg	0.036	0.022	0.006	0.0001	0.00017
10	Sample 3 after CaSi	0.037	0.022	0.006	0.0017	0.00017
13	Sample 4 after Fe2O3	0.039	0.017	0.006	0.0009	0.00008
17	Sample 5- after NiMg	0.037	0.0175	0.006	0.0004	0.00038

Table 3: Composition of Samples (Heat 3)

Time, min	Sample	Composition				
		C	Al	S	Ca	Mg
0	Sample 1- after Al	0.0389	0.051	0.005	0.0001	0.00008
5	Sample 2- after NiMg	0.0384	0.053	0.005	0.0001	0.00012
10	Sample 3 after CaSi	0.0416	0.054	0.005	0.0029	0.0001
16	Sample 4- After Fe2O3+ Mg	0.0404	0.051	0.005	0.0016	0.00034

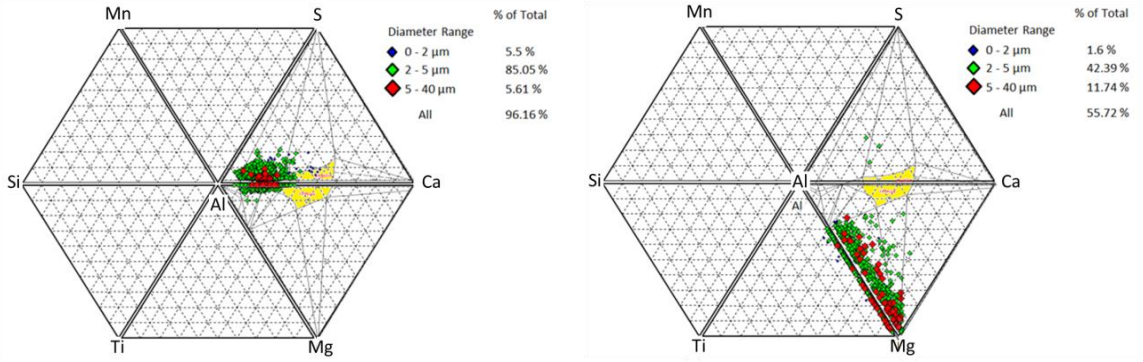

(a) (b)

Figure 6: Heat 2 inclusion composition for samples taken after calcium treatment and after reoxidation and addition of magnesium. (a) after calcium treatment, and (b) after reoxidation and addition of magnesium.

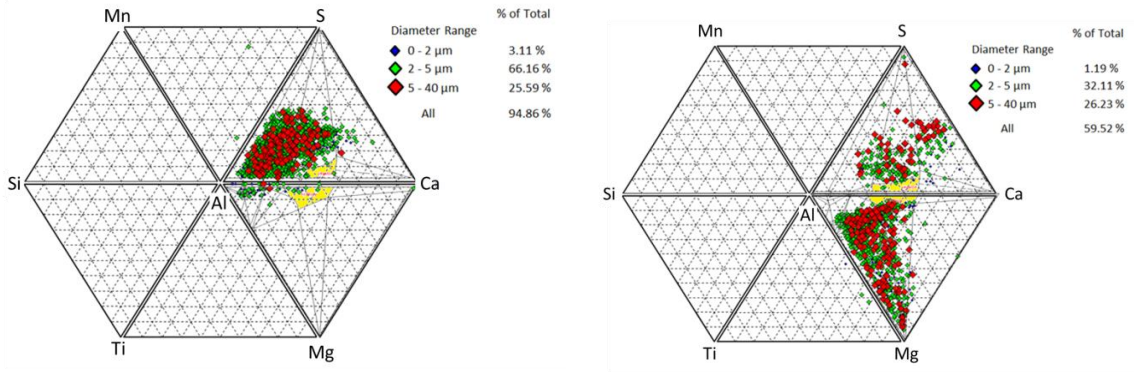

(a) (b)

Figure 7: Heat 3 inclusion composition for samples taken after calcium treatment and after simultaneous addition of magnesium and oxygen. (a) after reoxidation, (b) after addition of magnesium and oxygen.

Population Density Function

Industrial Trial

Lollipop samples were collected during a startup heat at different positions in the steelmaking process. Samples were taken from the ladle top at the end of calcium treatment and also from the tundish after different amounts of liquid steel had been poured. Table 4 shows the sampling locations during this heat.

Table 4: Sample Locations

Sample No.	Steel Treatment	Stage
1	After Ca addition	LMF
2	T1 (85% steel in ladle)	Tundish
3	T2 (75% steel in ladle)	
4	T3 (50% steel in ladle)	
5	T4 (10% steel in ladle)	

Samples were sectioned, polished and analyzed for inclusions using SEM with EDS capability. Post processing analysis was done using methodology described in [10]. Figure 8 shows the inclusion composition after calcium treatment and in the tundish at initial pouring time (position T1). During steel transfer, a shift in the inclusion population is observed in the direction of increasing alumina inclusions and the presence of fine alumina rich inclusions suggests that this change resulted from reoxidation.

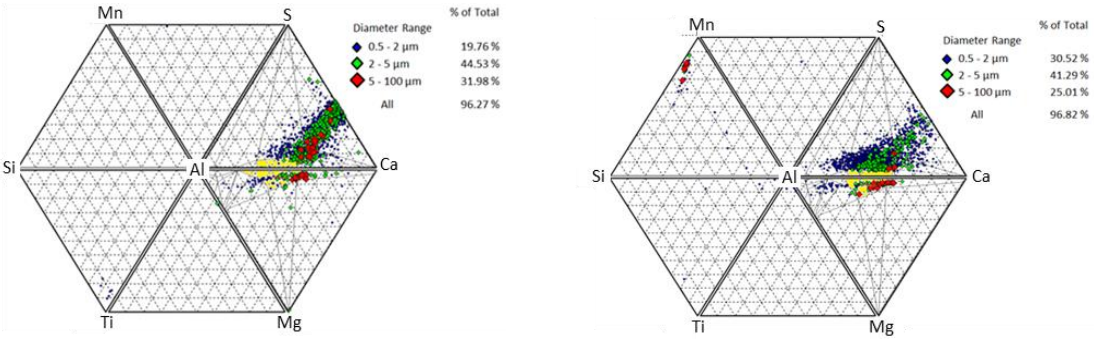

(a) (b)

Figure 8. Inclusion composition at final LMF and tundish. (a) final LMF (after Ca treatment), and (b) tundish (position T1). Presence of fine alumina inclusions in the tundish is evidence of reoxidation during transfer.

Figures 9a and 9b show the lnPDF-ln (inclusion diameter) plot for the size distribution of oxide inclusions in the respective samples. At LMF final, a linear size distribution is observed. During transfer of liquid steel to the tundish, the size distribution changes from linear to quadratic. The shift in the shape agrees with the model by Ende [1] and suggests that a linear distribution is present when the inclusions are in kinetic equilibrium with the steel and under active nucleation and growth, the distribution is quadratic. This change in the shape of the distribution from linear to quadratic therefore resulted from liquid steel reoxidation.

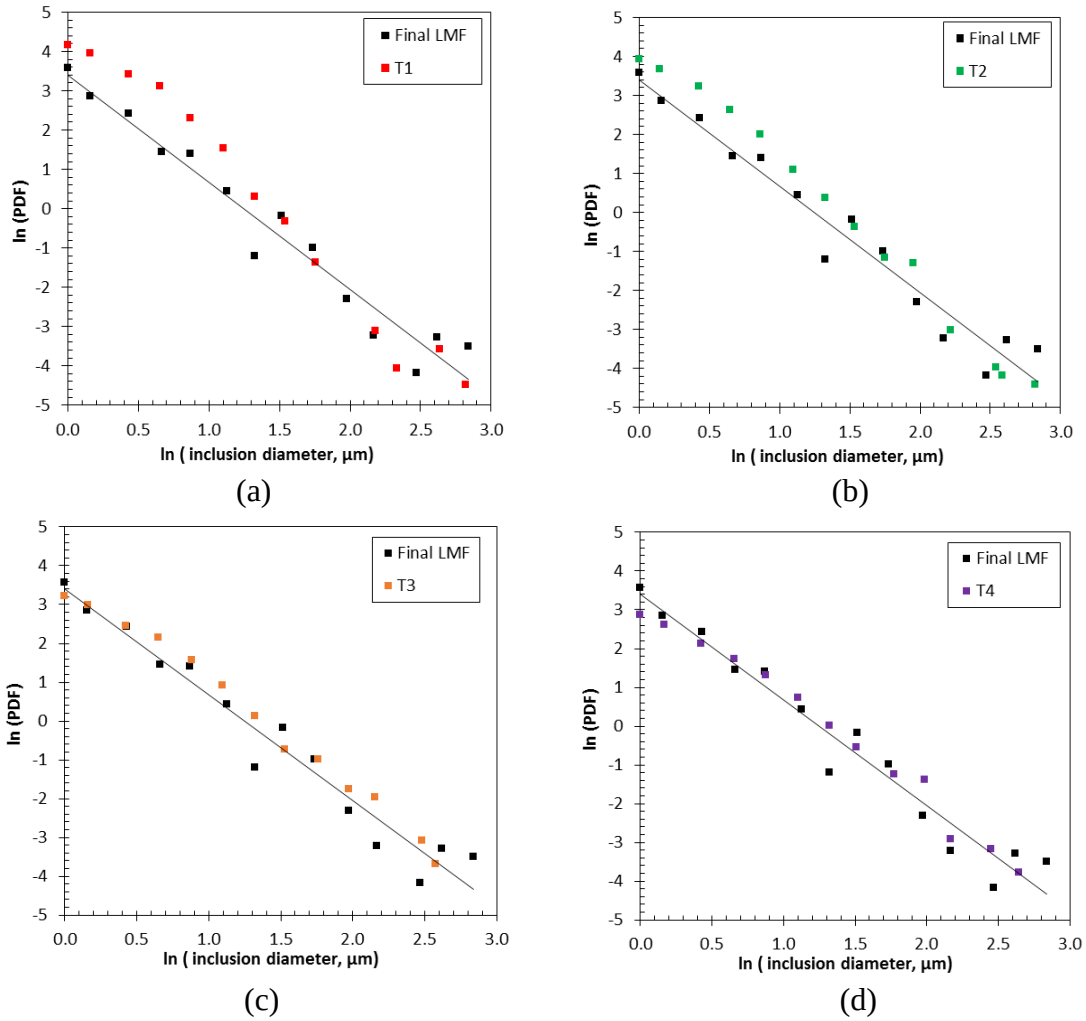

Figure 9: ln-ln plot of the size distribution of oxide inclusions observed in tundish samples taken from a startup heat. (a) position 1, (b) position 2, (c) position 3, and (d) position 4.

Figure 10 shows the change in β^2 with α for the tundish samples. The results show a decreasing value of β^2 with increasing α. A comparison of the observed result to the model by Eberl et al [1] suggests Ostwald ripening as the cause of the shape change in the tundish sample.

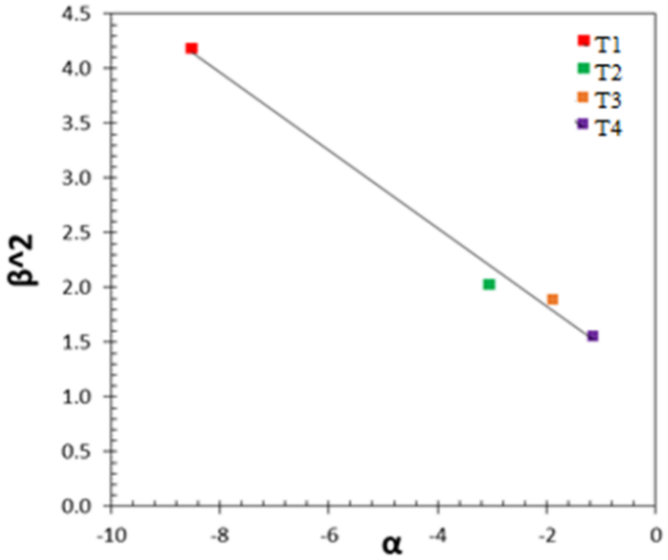

Figure 10: Plot of β^2 and α for samples taken from the tundish. The observed negative slope suggests the shape change resulted from Ostwald ripening.

Laboratory Experiment

The PDF method was also applied to the collected laboratory samples to observe possible changes in the inclusion size distribution for spinels before and after reoxidation. Because the oxygen content at the start of heat 2 was relatively high (400ppm oxygen) compared to heat 3 (173ppm oxygen), only results for heat three are shown. The higher oxygen content resulted in a higher number of alumina inclusions that made transformation to spinel after aluminum deoxidation difficult. Figure 11a shows the PDF of spinels before and after reoxidation while figure 11b shows the shape of the distribution in a ln-ln plot. The linear distribution for the spinel inclusions observed before reoxidation suggests that the inclusions were in equilibrium with the liquid steel prior to sample collection. After reoxidation, there was nucleation and growth and hence the quadratic shape. About 4 minutes was given between alloy addition and sample collection and the observed quadratic trend suggests that more time might have been required after reoxidation for the

inclusions to attain equilibrium. The results however, show that the spinel inclusions after reoxidation are larger in size and also more spherical. The larger size is possibly due to heterogeneous nucleation of spinel on the existing inclusion population and from the thermodynamic model, suggests that spinels are formed after the calcium aluminates. The spinel inclusion characteristics in both samples are summarized in table 5.

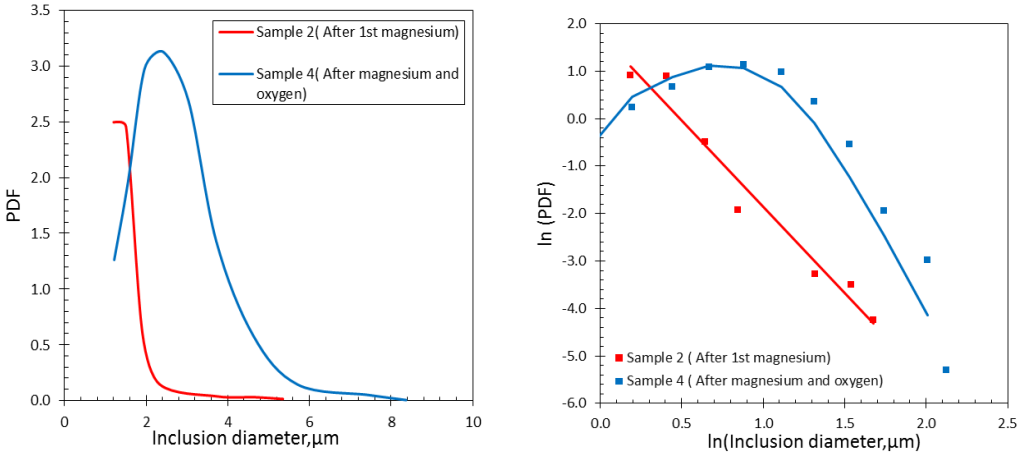

(a) (b)

Figure 11: Size distribution of spinel inclusions in heat 3. Linear size distribution of spinel inclusions observed before reoxidation suggests that the inclusions were in equilibrium with the steel. After reoxidation, a quadratic distribution is observed and the spinels are larger in size.

Table 5: Spinel Inclusion Characteristics (Heat 3)

Process Stage	Spinel inclusions	
	Size, µm	Aspect ratio
Before reoxidation	1.56	1.3
After reoxidation	2.82	1.17

CONCLUSION

The effect of reoxidation on the formation of spinel was investigated via laboratory heats and the method of population density function was applied to study the inclusion characteristics from industrial mini mill and laboratory samples.

The results showed that at low magnesium in steel solution (about 1ppm) complex spinel

calcium aluminate inclusions are formed. Single phase spinel inclusions were observed to form when the magnesium content was increased to about 4ppm.

Application of population density function (PDF) to industrial mini mill samples showed a linear distribution after calcium treatment. The shape of the size distribution transformed to quadratic due to liquid steel reoxidation. Both distributions were in agreement with literature and suggest inclusion-steel equilibrium after calcium treatment and active nucleation in the tundish. The size distribution of spinel inclusions from the laboratory experiments showed that after reoxidation, the spinel inclusion size increased from about 1.5 μm before reoxidation, to 3 μm after reoxidation. This increase suggests that the spinel inclusions nucleated on existing inclusions.

REFERENCES

1. Evolution of Non-Metallic Inclusions in Secondary Steelmaking: Learning from Inclusion Size Distributions. Marie-Aline Van Ende, Muxing GUO, Enno Zinngrebe, Bart Blanpain, In-Ho Jung.

2. Crystal Size Distribution (CSD) in Rocks and the Kinetics and Dynamics of Crystallization I. Theory. Bruce D. Marsh.

3. Crystal Size Distribution (CSD) in Rocks and the Kinetics and Dynamics of Crystallization III. Metamorphic Crystallization. Katharine V. Cashman and John M. Ferry.

4. Deducing the Growth Mechanisms for Minerals from the Shapes of Crystal Size Distributions. D.D. Eberl, V.A. Drits, J. Srodon.

5. Inclusion Population Evolution in Ti-alloyed Al-Killed Steel during Secondary Steelmaking Process. Enno Zinngrebe, Corrie Van Hoek, Henk Visser, Albert Westendorp, and In-Ho Jung.

6. Morphology and growth of alumina inclusions in Fe-Al alloys at low oxygen partial pressure. M.A. Van Ende, M.X. Guo, E. Zinngrebe, R. Dekkers, J. Proost, B. Blanpain, and P. Wollants.

7. Measurement of Crystal Size Distribution. Michael D. Higgins.

8. An SEM/EDS Statistical Study of the Effect of Mini-Mill Practices on the Inclusion Population in Liquid Steel. Obinna Adaba, Marc Harris, Ronald J. O'Malley, Simon N. Lekakh, Von L.Richards.

9. Improved Methodology for Automated SEM/EDS Non-Metallic Inclusion Analysis of Mini-Mill and Foundry Steels", M. Harris, O. Adaba, S. Lekakh, R. O'Malley, and V. L. Richards, Proc. AISTech 2015, Cleveland, May 4-7, 2015, pp. 2315-2325.

10. Evolution of Non-Metallic Inclusions in Ultra Low Carbon Steel after Aluminum Deoxidation. Myuang-Duk SEO, Jung-Wook CHO, Kwang-Chun and Seon-Hyo.

11. On the Interpretation of Crystal Size Distribution in Magmatic Systems. Bruce D. Marsh.

12. Calcium Modification of Spinel Inclusions in Aluminum-Killed Steel: Reaction Steps. N. Verma, P.C Pistorius, R.J Fruehan, M.S. Potter, H.G. Oltmann, E.B, Pretorius.

SECTION

4. CONCLUSION

The formation and evolution of spinel inclusions in line pipe steels was investigated by studying samples taken from industrial mini mills and also conducted laboratory experiments. Analysis of industrial samples showed that spinel inclusions are first formed during the desulfurization process and by reactions between dissolved aluminum and ladle slag. These inclusions were modified by calcium after treatment to calcium magnesium aluminates and also observed was the formation of MgO rich and CaS inclusions. During the transfer of liquid steel from the ladle to the tundish, there was evidence of reoxidation by the appearance of fine alumina rich inclusions and the already present CaS inclusions seemed to act as a source of calcium to modify these new inclusions. Conducted laboratory experiments showed that spinel inclusions can be formed after reoxidation of liquid steel if there is sufficient magnesium in solution. From these experiments, spinels where formed when the magnesium content in steel was about 4ppm. Below this amount, complex spinel and calcium aluminate inclusions are formed. The observed spinel inclusions after reoxidation were also larger than those before reoxidation and this suggests the spinel inclusions grew form the existing inclusion population.

5. FUTURE WORK

5.1. FORMATION OF MgO INCLUSIONS DURING CALCIUM MODIFICATION OF SPINELS

Industrial studies showed the presence of MgO rich inclusions surrounded by a calcium aluminate layer after calcium modification of spinel inclusions (fig 5.1). These MgO rich inclusions are also detrimental to the casting process and mechanical properties of the product. Preliminary calculations done using the commercial thermodynamic software Factsage 6.4 showed that spinel inclusions are stable over a wide range of magnesium content in steel and during the calcium modification of MgO saturated spinel inclusions, these MgO inclusions can be produced. Figure 5.2 shows the results of calcium modification of spinel with steel containing different amounts of magnesium. The results however, need to be verified experimentally and the mechanism by which these inclusions are produced in steel determined

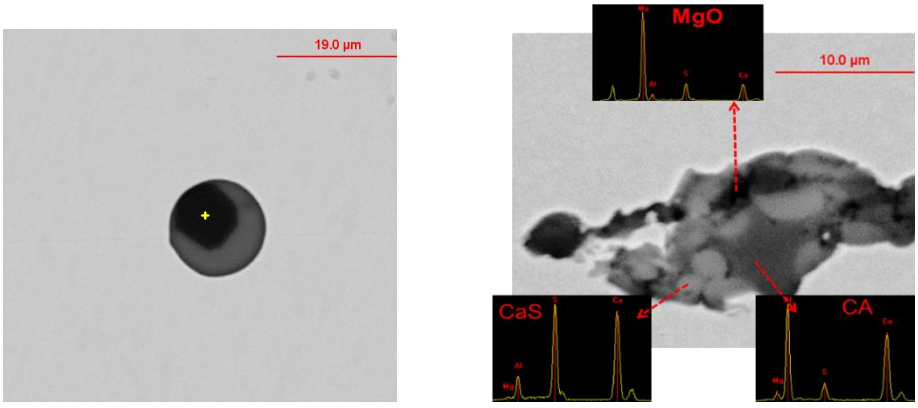

(a) (b)

Figure 5.1: SEM image of MgO rich inclusions observed after calcium treatment. (a) ladle sample, (b) coil sample. Figure shows that these inclusion types are detrimental to the casting process and mechanical property

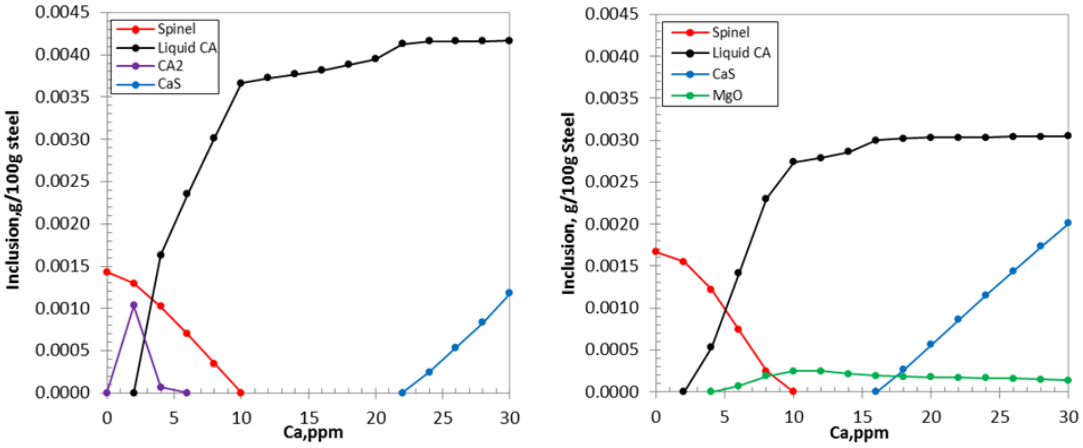

(a) (b)

Figure 5.2**:** Calcium modification of spinel. Calculation done with (a) 5ppm Mg in steel, (b) 14ppm Mg in steel, showing that MgO can persist after Ca treatment.

5.2. THE FORMATION OF SPINELS AFTER REOXIDATION

The conducted laboratory experiments only produced spinel inclusions after calcium treatment when magnesium was added. Most of the magnesium was observed to vaporize rather than stay in solution and thus did not agree with proposed reaction mechanism from literature. These experiments were however conducted without MgO saturated slags that can prevent magnesium vaporization. Also the atmosphere was not 100% argon as observed in steelmaking. The experiment therefore needs to be repeated and these factors taken into consideration.

5.3. CaS AS A SOURCE OF CALCIUM TO BUFFER REOXIDATION INCLUSIONS

CaS inclusions are typically not desired because of their clogging tendencies. However, the possibility of CaS to act as a source of calcium to buffer inclusions formed after reoxidation was observed in the industrial mini mill studies. Calcium has a low solubility in liquid steel and is mostly associated with inclusions. After reoxidation, new oxide inclusions are formed in the liquid steel and without a calcium source to modify these inclusions, the beneficial effects of calcium treatment are spoiled.

REFERENCES

1. M. Harris, O. Adaba, S. Lekakh, R. O'Malley, and V. L. Richards. "Improved Methodology for Automated SEM/EDS Non-Metallic Inclusion Analysis of Mini-Mill and Foundry Steels".

2. Y.Ren, L.Zhang, S. Li, W. Yang, Y. Wang. "Formation Mechanism of CaO-CaS Inclusions in Pipeline Steels".

3. Scott R. Story, Riad I. Asfahani. "Control of Ca Containing Inclusions in Al-Killed Steel Grades".

4. Hiroyasu Itoh, Mitsutaka Hino, and Shiro Ban-Ya."Thermodynamics on the Formation of Spinel Nonmetallic Inclusion in Liquid Steel".

5. B.Coletti, B.Gommers, C. Vercruyssen, B.Blanpain, P.Wollants, and F. Haers. "Reoxidation during Ladle Treatment".

6. Marc Rubat du Merac, Hans-Joachim Kleebe, Mathis M. Muller, and Ivar E. Reimanis. "Fifty Years of Research and Development Coming to Fruition;Unraveling the Complex Interactions during Processing of Transparent Magnesium Aluminate (MgAl2O4) Spinel".

7. Rick Meade. "Non-Destructive Evaluation of Low-frequency Electric Resistance Welded (ERW) Pipe Utilizing Ultrasonic In-Line Inspection Technology".

8. Ying Ren, Lifeng Zhang, and Shusen Li. "Transient Evolution of Inclusions during Calcium Modification in Linepipe Steels".

9. Zhiyin Dend, and Miaoyong Zhu. "Evolution Mechanism of Non-metallic Inclusions in Al-Killed Alloyed Steel during Secondary Refining Process".

10. Sima Aminorroaya, Hossein Edris, Mehrdad Fatahi. "Hook Crack in Electric Resistance Welded Line Pipe Steel".

11. Die Yang, Xinhua Wang, Guangwei Yang, Pengyuan Wei, and Jinping He. "Inclusion Evolution and Estimation during Secondary Refining in Calcium Treated Aluminum Killed Steels".

12. I.G. Saucedo, M. Alavanja, D. Phillipi "Characterization and prevention of hook cracks in tubular products".

13. N. Verma, P.C Pistorius, R.J Fruehan, M.S. Potter, H.G. Oltmann, E.B, Pretorius, "Calcium Modification of Spinel Inclusions in Aluminum-Killed Steel: Reaction Steps".

14. Jacques Poirier. “Fundamentals of Corrosion Behavior”.

15. J.Tan, B.A. Webler. “Inclusion Evolution after Controlled Reoxidation”.

16. P.A. Thornton. “ The Influence of Nonmetallic Inclusions on the Mechanical Properties of Steel: A Review”.

17. IN-HO Jung, Sergei A. Decterov, and Arthur D. Pelton. “A Thermodynamic Model for Deoxidation Equilibria in Steel”.

18. Lifeng Zhang, Brian G. Thomas. “Evaluation and Control of Steel Cleanliness”.
19. Jose Carlos S. Pires. “Modification of oxide inclusions present in aluminum-killed low carbon steel by addition of calcium”.

20. Shufeng Yang, Qiangqiang Wang, Lifeng Zhang, Jingshe Li, and Kent Peaslee. “Formation and Modification of MgO·Al2O3-Based Inclusions in Alloy Steels”.

21. Non-Metallic Inclusions in Steel. Ronald Kiessing.

22. Influence of Oxide Nature on the Machinability of 316L Stainless Steel. O. Bletton, R. Duet, and P. Pedarre.

23. Characteristics of Particle Size Distribution in Early Stage of Deoxidation. H. Suito and , H. Ohta.

24. The Shaping, Making, and Treating of Steels. R.J. Fruehan.

25. Rate of Reduction of MgO by Carbon. R.J. Fruehan.

26. Calcium and Magnesium thermodynamics in steel and its impact on secondary steelmaking: a computational thermodynamic approach. A. Costa e Silva.

27. Absorption of Non-Metallic Inclusions by Steelmaking Slags—A Review. Bruno Henrique Reis, Wagner Viana Bielefeldt, and Antônio Cezar Faria Vilela.

28. Fundamental Studies Related to the Mechanisms of Inclusion Removal from Steel. G.Hassal, and K.Mills.

29. Principles of Metal Refining. T. A. Engh, Christian J. Simensen, and Olle Wijk.

VITA

Obinna Menyelum Adaba was born in Lagos, Nigeria. In January 2010, he received his bachelor's degree in Metallurgical and Materials engineering from the University of Lagos, Nigeria.

Obinna began his Master's degree at Missouri University of Science and Technology in January 2013 and was introduced into the exciting world of steelmaking research by the Late Dr. Kent Peaslee. In summer of 2013, he began his research on non-metallic inclusions for the Peaslee Steel Manufacturing Research Center (PSMRC). During his time as a graduate research assistant for the center, he co-authored in one and wrote two papers for publication in conference proceedings. He also worked as a research and development intern in summer of 2015 for ArcelorMittal global R&D.

While pursuing his degree, he was privileged to serve the African Students Association first as a student council representative and later as president. He was also a member of Materials Advantage, American Foundry Society (AFS), and Alpha Sigma Mu. Obinna earned his M.Sc degree in Metallurgical engineering in December 2015.